1-1-2014

Longitudinal Change In Regional Cortices And Fluid Intelligence

Peng Yuan
Wayne State University,

LONGITUDINAL CHANGE IN REGIONAL CORTICES AND FLUID INTELLIGENCE

by

PENG YUAN

DISSERTATION

Submitted to the Graduate School

of Wayne State University,

Detroit, Michigan

in partial fulfillment of the requirements

for the degree of

DOCTOR OF PHILOSOPHY

2014

MAJOR: PSYCHOLOGY

Approved by:

_____

Advisor Date

_____

_____

_____

_____

TABLE OF CONTENTS

LIST OF TABLES

LIST OF FIGURES

Chapter I

Introduction

Over a century ago, Spearman noticed positive correlations among scores on diverse cognitive tasks, and proposed the hypothesis of general intelligence, or *g* factor, to explain the observed commonality among mental abilities (Spearman, 1904, 1927). According to Spearman's hypothesis, the *g* factor is an expression of commonality among diverse cognitive abilities. According to the general intelligence theory, persons with higher *g* scores are expected to perform better on a variety of different tests. Decades later, Spearman's student Raymond Cattell proposed that intelligence is not a unitary entity, as he introduced the concepts of fluid (G*f*) and crystallized intelligence (G*c*) as independent components of general intelligence (Cattell, 1943). The G*f*-G*c* theory was further refined by Cattell's student John Horn (Horn & Cattell, 1966), who introduced additional second-order factors, such as visualization capacity, perceptual speed, and fluency. Fluid intelligence refers to the capacity for logical reasoning and problem-solving independent of acquired knowledge (Cattell, 1971). G*f* is typically evaluated with nonverbal tests such as the Cattell Culture Fair IQ test (CFIT, Cattell & Cattell, 1973) and the performance subscale of the Wechsler Adult Intelligence Scale (WAIS, Wechsler, 1958), which require implementation of reasoning skills based on novel information but not on acquired knowledge. Crystallized intelligence (G*c*), on the other hand, is the capacity to make use of acquired and acculturated knowledge, is affected by individual's education and cultural experience, and can be assessed by tests of vocabulary and general knowledge. Although G*f* and G*c* are distinct factors of intelligence, they correlate with each other (Carroll, 1993), usually greater than $r = 0.3$ (Flanagan & McGrew, 1998; Li, et al., 2004).

Fluid and crystalized components of intelligence exhibit different age-related trajectories of change (Desjardins & Warnke, 2012; McArdle, Ferrer-Caja, Hamagami, & Woodcock, 2002). Fluid intelligence (*Gf*) increases rapidly during childhood and adolescence, peaks in early adulthood and then declines substantially across the later part of the life span. Age-related differences were reported in various indices of G*f*, and G*f* has become viewed as an age-vulnerable or age-sensitive ability (Horn & Blankson, 2005). Crystalized intelligence indices show higher scores in older children compared to their younger counterparts, and *Gc* is thus assumed to rise in the course of early development, just as the fluid intelligence does. However, as indicated in a longitudinal study, G*c* does not decline in healthy adults, but it may increase further when G*f* peaks and starts to decline (McArdle, Hamagami, Meredith, & Bradway, 2000).

Fluid intelligence is associated with many types of cognitive operations and shows a strong relationship with executive functions (Unsworth, et al., 2009). Executive functions are referred to as "*an umbrella term comprising a wide range of cognitive processes and behavioral competencies which include verbal reasoning, problem-solving, planning, sequencing, the ability to sustain attention, resistance to interference, utilization of feedback, multitasking, cognitive flexibility, and the ability to deal with novelty*" (Chan, Shum, Toulopoulou, & Chen, 2008). A study of patients with frontal lesions revealed that for some typical executive functioning tasks such as Wisconsin Card Sorting Test and verbal fluency, executive functioning scores highly correlated with fluid intelligence: $r = 0.61$ for WCST and 0.56 for verbal fluency, both $p < 0.001$ (Roca, et al., 2010). Working memory capacity, a component of executive functions, is also highly correlated with fluid intelligence (Colom, Rebollo, Palacios, Juan-Espinosa, & Kyllonen, 2004; de Jong & Das-Smaal, 1995; Engle, Tuholski, Laughlin, & Conway, 1999; Kyllonen & Christal, 1990). Blair used

fluid intelligence, working memory and executive function as interchangeable terms that are distinctly different than crystalized cognition (Blair, 2006). Although the isomorphisms of executive function, working memory and G*f* are not universally accepted, all concur that executive functions, working memory and G*f* are strongly related (Burgess, Braver, & Gray, 2006; Garlick & Sejnowski, 2006; Heitz, et al., 2006), with the magnitude of the correlation between G*f* and working memory attaining values up to $r = 0.8$ (Kyllonen & Christal, 1990).

Just as executive functions are related to the volume and thickness of the prefrontal cortex (for review, see Yuan & Raz, 2014), fluid intelligence also is associated with the integrity of frontal lobes. For example, patients with prefrontal lesions exhibit impaired performance on CFIT (Roca, et al., 2010). In addition to the frontal lobe, lesions in parietal cortex also result in deficits in fluid intelligence (Woolgar, et al., 2010). In functional neuroimaging studies, increased activation in frontal and parietal cortex is observed during fluid reasoning (Masunaga, Kawashima, Horn, Sassa, & Sekiguchi, 2008; Prabhakaran, Smith, Desmond, Glover, & Gabrieli, 1997) and fluid analogies (Geake & Hansen, 2005). The anterior cingulate, a region that is responsible for selection of responses and inhibition of alternative actions (Braver, Barch, Gray, Molfese, & Snyder, 2001; Turken & Swick, 1999), shows increased activation in tasks requiring fluid intelligence (Duncan, et al., 2000; Geake & Hansen, 2005). In the temporal lobe, many regions support diverse cognitive operations that are relevant to Gf. Some regions, such as posterior superior temporal gyrus (Luo, et al., 2003), inferior and middle temporal gyri (Goel & Dolan, 2004; Knauff, Mulack, Kassubek, Salih, & Greenlee, 2002), as well as fusiform gyrus (Goel & Dolan, 2004; Luo, et al., 2003), have been linked to reasoning. Specifically, the fusiform area is involved in pattern recognition (Gauthier, et al., 2000; Tarr & Gauthier, 2000); the inferior temporal gyrus

appears to be dedicated to high-level visual processing and memory (Miyashita, 1993); and portions of the superior and middle temporal gyri participate in processing of auditory information (Jancke, Wustenberg, Scheich, & Heinze, 2002).

Jung and Haier reviewed a number of structural, PET and fMRI studies of reasoning intelligence, and proposed the Parieto-Frontal Integration Theory (P-FIT) to account for the inter-person difference in intelligence and reasoning tasks (Jung & Haier, 2007). Jung and Haier's P-FIT model describes a network of brain regions that includes the dorsolateral prefrontal cortex, the inferior and superior parietal lobule, the anterior cingulate, and some areas within the temporal and occipital lobes, which are hypothesized to be involved in fluid reasoning tasks. The P-FIT model assumes the following roles in reasoning and intelligence: The temporal and occipital regions are involved in the early processing of sensory information; then this information is fed to the parietal cortex, which interacts with frontal areas; frontal cortex generates the best solution to a given problem; and anterior cingulate constrains the selected response and inhibits other competing process. In light of the P-FIT model, the current study evaluated the relationship between fluid intelligence and frontal, parietal, temporal, and anterior cingulate cortices.

Contemporary *in vivo* neuroimaging makes it possible to investigate brain structures of healthy human adults, and it has revealed substantial morphological alterations in prefrontal and parietal cortices with increasing age. Significant age-related shrinkage in the lateral prefrontal and/or orbito-frontal cortices is suggested by studies of regional brain volumes (Raz, Ghisletta, Rodrigue, Kennedy, & Lindenberger, 2010; Raz, et al., 2005). Some studies reported significant age-related difference in the volume of superior parietal cortex (Raz, et al., 1997), although in some other studies, the age difference in parietal cortex was non-significant (Raz, et al., 2004).

As observed in a longitudinal study with a mean follow-up interval of about 5 years, the shrinkage rate could be as high as 0.91% per year in lateral prefrontal cortex, 0.85% per year in orbito-frontal cortex and 0.87% annually in the inferior parietal lobule, corresponding to effect sizes (Cohen's *d*) of 0.92, 0.79 and 0.89, respectively, for five-year mean changes (Raz, et al., 2005). However, other studies using same measurement methods but shorter follow-ups replicated significant shrinkage only in orbito-frontal (with effect sizes of 0.41 and 0.42 over two consecutive intervals) but not in lateral prefrontal cortex, although individual differences in change rates were observed in all of these samples (Raz, et al., 2010). Besides the volume of gray matter, age-related cortical thinning in prefrontal and parietal cortices is also confirmed by studies measuring cortical thickness (Fjell, Westlye, et al., 2009; Salat, et al., 2004). Based on the findings of cortical thickness and volume, the vulnerability of PFC has been proposed, as the age effects on PFC are greater than age effects on the other neocortical regions (Fjell, Westlye, et al., 2009; Raz, et al., 1997; Raz & Rodrigue, 2006; Resnick, Pham, Kraut, Zonderman, & Davatzikos, 2003).

In cross-sectional studies, positive correlations have been reported between fluid intelligence and frontal cortex volume in healthy adults (Colom, et al., 2009; Gong, et al., 2005; Schretlen, et al., 2000). As summarized in a meta-analysis study, larger prefrontal volume or thickness is also associated with better executive functioning (Yuan & Raz, 2014), which overlaps to a large extent with fluid intelligence. In addition, the G*f*-cortex relationship is also found in parietal and temporal cortices, although the clusters of significant voxels in parietal regions were much smaller than the clusters in frontal lobe (Colom, et al., 2009).

In contrast to cross-sectional investigations of associations between age-related differences in brain and cognition, longitudinal studies of the change in G*f* and cortical size are

rare. A cross-sectional approach to studying age-related change is not informative in this regard, because in an age-heterogeneous sample, it is difficult to distinguish individual-level change from the age-related difference at population-level (Hofer & Sliwinski, 2001; Lindenberger & Pötter, 1998). The estimates of longitudinal mediation based on cross-sectional design can be biased (Maxwell & Cole, 2007), as the age-related variance revealed by cross-sectional data do not describe dynamic causal processes that can only be revealed in longitudinal analyses (Lindenberger, Von Oertzen, Ghisletta, & Hertzog, 2011; Raz & Lindenberger, 2011). In order to overcome the limitations of a cross-sectional design, the current study aimed to evaluate the relationship between longitudinal change in G*f* and longitudinal change in prefrontal and parietal cortices in a sample of middle-aged and older healthy adults.

The current study tried to address the following questions. First, how does G*f* change over time, and are there individual differences in change? Second, how do the volume and cortical thickness of prefrontal and parietal cortices change over time, and do the change trajectories differ among individuals? What is the shape of the change trajectories, i.e., does shrinkage accelerate with age? Third, are the baseline values and rates of change in G*f* related to the parameters of trajectory (i.e., initial value and rate of shrinkage) of regional volume or cortical thickness change?

Specifically, we hypothesized that G*f*, but not G*c*, would decline with age. Older age at baseline was expected to be associated with lower G*f* scores at baseline. At the same time, we hypothesized that older age would be associated with thinner prefrontal and parietal cortices at baseline. Furthermore, better baseline G*f* performance was expected to be associated with

thicker prefrontal and parietal cortices at baseline. Steeper decline in G*f* was hypothesized to be associated with faster thinning of prefrontal and parietal cortices.

In longitudinal studies, participants' performance can improve because of repeated exposure to tests. Practice effects have been evidenced in fluid intelligence (Rabbitt, Diggle, Holland, & McInnes, 2004), processing speed (Ferrer, Salthouse, McArdle, Stewart, & Schwartz, 2005), as well as memory (Ferrer, et al., 2005; Salthouse, Schroeder, & Ferrer, 2004), which can persist for several years (Salthouse, et al., 2004). It is possible that the rate of age-related decline could be underestimated if practice effects in the longitudinal data are not taken into account (Ferrer, et al., 2005; Rabbitt, Diggle, Smith, Holland, & Mc Innes, 2001). The current study tried to separate the practice gain and age-related longitudinal change in cognitive abilities. After controlling for practice effects, we were able to assess longitudinal change in fluid intelligence and crystallized intelligence.

Chapter II

Methods

Participants

Participants were healthy volunteers from the metropolitan Detroit area, who attained a minimum of high school education. They were native English speakers and were strongly right-handed (75% and above on the Edinburgh Handedness Questionnaire; (Oldfield, 1971). Individuals who reported a history of cardiovascular disease, neurological or psychiatric conditions, diabetes, head trauma with a loss of consciousness for more than 5 min, thyroid problems, drug and alcohol problems were excluded from participation in the study. Persons who were taking anti-seizure medication, anxiolytics, or antidepressants were excluded, too. Mini Mental State Examination (MMSE) (Folstein, Folstein, & McHugh, 1975) and Geriatric Depression Questionnaire (CES-D) (Radloff, 1977) were used to exclude probable individuals of dementia and depression, and only those who scored at least 26 on MMSE and below 16 on CES-D were admitted in the study. All participants provided informed consent for participation in this study, which was approved by university human investigations committee. There were 76 participants age 49 years and older eligible for the longitudinal study, 46 of whom returned for at least one follow-up. The participants who returned for follow-ups did not differ from the other participants in age or education (both $p > 0.2$). However, the 46 returning participants had higher MMSE than 30 participants who did not return for follow-up measures: $M \pm SD$: 28.8 ± 1.1 vs. 28.1 ± 1.0, t (74) = 3.056, p = 0.003. Only the 46 returning participants were included in the current study. The sample descriptive statistics are presented in Table 1.

Cognitive measures

Fluid intelligence. The Cattell Culture Fair Intelligence Test (CFIT, Form 3B, Raymond Bernard Cattell & Cattell, 1973) was administrated to measure fluid intelligence. Four subtests were administrated, each of which consisted of 10 to 14 nonverbal reasoning problems of a wide range of difficulty. The subtests covered different abstract reasoning domains such as detecting similarity in designs, completing matrices, and solving nonverbal syllogisms. Participants had to derive the rules required to solve the problems. Subjects were allowed to finish the entire test, but the items that had been completed at a certain limited time (2.5 to 4 minutes for each subtest) were noted. The indices of performance are the numbers of total correct items across four subtests, both timed and untimed.

Crystalize intelligence. G*c* was evaluated by vocabulary scores (V-2 and V-3) from the Educational Test Services Kit of Factor-Referenced Tests (Ekstrom, French, Harman, & Dermen, 1976). The subtest V-2 consisted of 18 items and subtest V-3 consisted of 24 items, all of which were 5-choice synonym tests. Participants were allowed to finish the entire tests, but the items that had been completed at 4 minutes for V-2 and 6 minutes for V-3 were noted. Subjects were instructed not go guess unless they could eliminate one or more answer choices as wrong. The indices of performance were the numbers of correct items minus 25% of incorrect items, separately for V-2 and V-3, both timed and untimed.

Processing speed (PS). Processing speed was assessed by letter comparison and pattern comparison tests (Salthouse & Meinz, 1995). The letter comparison task consisted of pairs of letter strings and the pattern comparison task consisted of pairs of line patterns. Participants

were required to make rapid judgments about whether two sets of stimuli were the same or different. The numbers of correct responses served as indices of performance on both tests.

Processing speed, fluid and crystalized intelligence were measured at each of the four occasions. The scores were standardized according to the means and standard deviations at baseline.

MRI protocol

Imaging was acquired on the same 1.5 Tesla Siemens Magnetom Sonata MRI system (Siemens Medical Systems, Erlangen, Germany) at Detroit Medical Center for all four waves. The cortical surface was reconstructed from a T1-weighted magnetization-prepared rapid gradient-echo (MPRAGE) sequence acquired in the coronal plane with the following parameters: repetition time (TR) = 800 ms, echo time (TE) = 3.93 ms, inversion time (TI) = 420 ms, field of view (FOV) = 192×192 mm, acquisition matrix = 256×256 mm, flip angle = 20°, and voxel size = 0.75×0.75×1.5 mm^3, 144 slices acquired in the coronal plane.

Image processing

To extract reliable cortical thickness and volume estimates, images were semi-automatically processed using FreeSurfer's longitudinal stream (Reuter, Schmansky, Rosas, & Fischl, 2012). A within-subject template was created for each individual subject (Reuter & Fischl, 2011; Reuter, Rosas, & Fischl, 2010), and subsequent processing were performed using the common information from the template, thus increasing the reliability and statistical power (Reuter, et al., 2012). The white matter and gray matter surfaces reconstructed from Freesurfer were inspected by the author (PY) and manually edited if necessary. All cases required manual

editing in orbito-frontal or/and temporal regions, e.g., removing dura and orbit that were wrongly classified as gray matter. Two cases needed manual removal of skull from the dorsal prefrontal cortex. Cortical thickness was computed as the average distance between pial surface and gray/white matter boundary within each region of interest (ROI).

Selection of ROIs for analysis

In Freesurfer, the cortex in each hemisphere is divided into 34 neuroanatomically labeled regions (Desikan, et al., 2006; Fischl, et al., 2004). Some of them were selected to constitute 6 ROIs in each hemisphere. The volume and cortical thickness of each ROI were calculated from Freesurfer output. I selected ROIs with theoretical propositions of P-FIT in mind. The selected FS labels and ROIs formed from them were as follows:

a. Middle PFC (MF): including *caudal middle frontal gyrus, rostral middle frontal gyrus.*
b. Inferior PFC (IF): including *pars-opercularis, pars-orbitalis, and pars-triangularis.*
c. Parietal cortex (PC): including *superior parietal, inferior parietal, supramarginal gyri.*
d. Anterior cingulate cortex (ACC): including *caudal anterior cingulate, rostral anterior cingulate.*
e. Temporal cortex (TC): including *superior temporal, middle temporal, inferior temporal and fusiform gyri*.
f. Visual cortex (VC): consisted of the *pericalcarine* area.

The definition of MF, IF, PC, TC and ACC tried to cover the frontal, parietal, temporal and cingulate areas proposed in Jung-Haier's P-FIT model. VC was supposed to be unrelated to intelligence, and served as a control area. Because the target cognitive index in this study, G*f*

represented a confluence of many cognitive operations, it was appropriate to aggregate specific anatomical regions into larger entities. All such agglomerations were tested with Confirmatory Factor Analysis.

Statistical analyses

Confirmatory factor analysis (CFA) on the structures of PFC and PC. The cortical thickness and volume of each region at baseline were regressed on age, and the residual values were used in CFA. CFAs were conducted to test whether the inclusions of the sub-regions in prefrontal cortex and parietal cortex are proper. Models were estimated using FIML (full-Information maximum likelihood) method. Missing cases were handled under the MAR (missing at random) assumption. CFA on PFC started from a measurement model that included measures of caudal middle frontal gyrus, rostral middle frontal gyrus, pars-opercularis, pars-orbitalis, and pars-triangularis (Figure 1a). Alternatively, the measures in superior frontal gyrus and frontal pole were added to examine whether the inclusion of superior frontal gyrus and/or frontal pole could make better fit (Figure 1b, 1c, 1d). Additionally, we split PFC into two regions, MF and IF, and checked whether the measurement model would fit better (Figure 1e). Similarly, CFA on PC started from a measurement model that included measures of superior parietal, inferior parietal, and supramarginal gyri (Figure 2a). An alternative measurement model with precuneus included was also examined (Figure 2b).

Measurement models of cortical thickness and volume. Two competing measurement models regarding cortical thickness were tested using the cortical data at baseline. In the 6-factor measurement model, the cortical thickness in each of the 6 ROIs (MF, IF, PC, ACC, TC and VC)

were presumed to be directly affected by age (Figure 3a). The 1-factor measurement model reflected the possibility that all measures of the regional cortical thickness formed one latent factor, directly affected by age (Figure 3b). This single-factor measurement model was specified to test the possibility that age-associated variance in regional cortical thickness could be explained by one single factor, without specifying the reasons and mechanisms that might contribute to in coherence common (e.g., developmental influences, or commonality of measurements). Similarly, 6-factor and 1-factor measurement models on ROI volume were also compared.

Latent growth curve modeling of longitudinal change. Latent growth curve (LGC) modeling was used to estimate the trajectories of change in G*f*, G*c*, and the cortical thickness and volume of each ROI. The analyses were conducted using *Mplus* software. The intercept (INT) and slope (SLP) of change were separately estimated in G*f* (Figure 4), G*c* (Figure 5), MF, IF, PC, ACC, TC and VC (Figure 6). Their associations with age were also assessed. Before conducting structural equation modeling (SEM), each of the cognitive and cortical measures was standardized according to the mean and standard deviation at baseline. Age as centered at 65 years old and scaled as units of decade.

Modeling practice effect. In the current study, we modeled the practice effect by introducing variables that indicated magnitude of practice gains. In Figures 4 and 5, the variables *re-test2, re-test3* and *re-test4* respectively represented the levels of previous exposure to particular cognitive tasks at the first, second and third follow-ups. They were defined as *k*-1, where it was the *k*-th time that the G*f* or G*c* test was longitudinally administered. For example, if

a subject participated at baseline and at the 1st and 3rd follow-ups, but skipped the 2nd follow-up, then *re-test2* = 1 and *re-test4* = 2.

Chapter III

Results

Confirmatory factor analysis (CFA) on the structures of PFC and PC.

CFA were conducted to examine whether combining individual sub-regions of dorsal prefrontal cortex (PFC) and parietal cortex (PC) was proper. The cortical thickness and volume of each region at baseline were regressed on age, and the standardized residual values were used in CFA. CFA on PFC began with a measurement model that included measures of caudal middle frontal gyrus, rostral middle frontal gyrus, pars-opercularis, pars-orbitalis, and pars-triangularis (model a, figure 1). Alternatively, the measures in superior frontal gyrus and/or frontal pole were added (models b, c, and d, figure 1). Additionally, we also tested a measurement model (model e, figure 1) in which DPFC was split into two factors: middle frontal gyrus (MF) and inferior PFC (IF). i.e., MF included caudal middle frontal gyrus and rostral middle frontal gyrus; IF included pars-opercularis, pars-orbitalis, and pars-triangularis. The regional cortical thickness and volume were separately examined.

AIC and BIC served as primary indices of model fit. When two models had similar AIC and BIC, the normed chi-square ($\chi 2/df$) would be referred. As listed in table 2 and table 3, the inclusion of superior frontal gyrus and/or frontal pole did not result in a model that fit better than the basic model. Therefore, superior frontal gyrus and the frontal pole were not included as part of the ROI of DPFC. Furthermore, splitting DPFC into MF and IF resulted in better model fit than the basic model, as indicated by smaller normed chi-square. Thus, in further analyses, MF and IF would be treated as two individual latent regions.

Similarly, CFA on PC started from a measurement model (model a, figure 2) that included measures of superior parietal, inferior parietal, and supramarginal gyri. An alternative measurement model with precuneus included was also examined (model b, figure 2). As listed in table 4 and table 5, the inclusion of precuneus did not result in better fit than the basic model, as indicated by smaller AIC and BIC. Thus, precuneus was not included as part of the ROI of PC.

Measurement models of cortical thickness and volume

Competing measurement models regarding regional cortical thickness, surface area and ROI volume were tested using regional size data at baseline. In each model of cortical thickness, the cortical thickness of each ROI was calculated by averaging cortical thickness values across the sub-regions included in the ROI, weighted by the surface areas of sub-regions.

As listed in table 6, the 6-factor measurement models had similar AIC and BIC with 1-factor model, but smaller normed chi-square, smaller SRMR and smaller RMSEA than the 1-factor models. The 1-factors model did not fit better, so the 6-factor measurement models were retained for further analyses. As indicated by the measurement models, smaller cortical thickness and smaller volume were associated with older age, whereas surface area was unrelated to age. Thus, we focused on cortical thickness and volume in examining the relationship with G*f*, which is an age-sensitive cognitive measure.

Latent growth curve modeling of longitudinal change

Latent growth curve (LGC) modeling was used to estimate the trajectories of change in G*f*, G*c*, and the cortical measures of MF, IF, PC, ACC, TC and VC.

LGC of cognitive measures.

In the latent growth curve model of G*f* (Figure 4), the performance on G*f* task varied with the number of previous tests (estimate = 0.180, p = 0.043), revealing that G*f* performance can benefit from repeated exposure (re-test effect). The effect of age on the growth intercept was significantly negative (estimate = -0.470, p = 0.002), indicating that advanced age was associated with poorer performance at baseline. After controlling for the repeated exposure (practice) effect, the slope of G*f* change was significantly negative (estimate of Slope = -0.718, p = 0.016), i.e., the G*f* performance declined over time (figure 7). There was also a significant age effect on slope of G*f* change (estimate = -0.334, p = 0.040), suggesting that the decline of G*f* is accelerated with age. The variance of slope was not significant, indicating the lack of individual differences in G*f* decline over time.

For the untimed G*f* scores, the effect of age on baseline performance was still significantly negative (estimate = -0.326, p = 0.019). After controlling for the repeated exposure (practice) effect, the slope of G*f* change was significantly negative (estimate of slope = -1.071, p = 0.002). However, the age effect on slope of G*f* change was no longer significant (estimate = -0.283, p = 0.233). Thus, in contrast to the significant acceleration of longitudinal decline for the timed scores, the untimed scores showed no such effect, suggesting that the acceleration of G*f* decline observed in timed scores might result from age-related slowing.

To test this hypothesis, we examined processing speed (PS) in the same LGC framework. The PS factor was measured by letter comparison and pattern comparison tasks (figure 8). Advanced age was associated with poorer PS at baseline (estimate = -0.468, p = 0.003), but the

slope of PS change was not significant. When G*f* was modeled together with PS, and their intercepts and slopes were allowed to correlate, the age effect on timed G*f* change slope became non-significant (estimate = -0.297, p = 0.090). Notably, the estimated magnitude of age effect on G*f* slope with PS controlled was very close to the estimated value for untimed G*f* (-0.297 vs. -0.283). Given the small sample size of the current study, it is possible that the non-significance could be due to low power. In the combined model of G*f* and PS, a positive correlation was found between baseline scores on timed (estimate = 0.311, p = 0.012), but not untimed (estimate = 0.186, p = 0.107) G*f* and PS. The non-significant correlation could also result from low power that was related to sample size. No relationship was found between the slopes of fluid intelligence and processing speed.

In contrast to G*f*, in the latent growth curve model of G*c*, directional paths were not significant (all *p's* > 0.3), suggesting the absence of practice effect on the G*c* task, and the independence of baseline G*c* from age (figure 9). The estimate of G*c* slope change did not significantly differ from zero (estimate = 0.156, p = 0.271), indicating that G*c* did not significantly change over time. Similar to the timed scores for vocabulary, none of the directional paths was significant in the untimed data. When G*f* and G*c* were entered together into one model (Figure 10), a significant positive correlation was found between the intercepts of G*f* and G*c* (estimate = 0.308, p = 0.005).

LGC of change in cortical thickness, volume, and surface area.

Table 7 listed the results of LGC models on ICV-adjusted ROI volumes. Age was centered at 65 years and scaled as units of decades. The time intervals were also scaled in decades. The

volumes in two hemispheres served as two indicators of the latent variables of ROI volume. The slopes were significantly negative for all the investigated ROIs except VC, although there was no significant slope variance. Age was negatively associated with baseline volumes of MF, IF, PC and VC, but not with slopes (Figures 11, 12, 13, 14, 15, 16, respectively). These results evidenced longitudinal shrinkage in MF, IF, PC, ACC and TC but not VC, as indicated by the 95% confidence intervals. No significant difference in the magnitude of age differences in baseline volume was found across regions.

Table 8 listed the results of LGC models on ROI cortical thickness. Similar to the LGC on volume measures, the age effect on baseline cortical thickness was significant in all ROIs except for ACC (Figures 11, 12, 13, 14, 15, 16, respectively). However, the slope was not significant in MF, ACC, and in VC, the direction of slope was even reversed. None of the regions demonstrated a significant slope-intercept correlation: $-0.147 < r < 0.178$ for volume and $-0.049 < r < 0.261$ for thickness, all $p > 0.05$.

Additionally, the latent changes in regional surface area were modeled. As previously tested in the measurement model, baseline surface areas of MF, IF, PC, ACC, TC and VC were unrelated to age. However, surface areas in all these regions longitudinally reduced. The shrinkage rates were -0.368, -0.501, -0.380, -0.281, -0.376 and -0.245 respectively for MF, IF, PC, ACC, TC and VC, all $p's < 0.001$.

LGC models for G*f*, G*c*, PS, and ROI measures were merged into combined models to examine possible associations between intercept and slope of cortical structural and cognitive

change. No significant associations were found between slopes and intercepts of changes in G*f*, G*c*, PS and changes in the examined ROI volume and cortical thickness (Table 9).

Chapter IV

Discussion

The current 4-wave study modeled longitudinal change in fluid intelligence, crystallized intelligence, processing speed and regional cortical thickness and volume in middle aged and aged healthy human adults. Longitudinal decline was observed in G*f*. Advanced age was associated with poorer G*f* at baseline and a steeper decline rate. In contrast, neither longitudinal decline nor age differences at baseline were observed in G*c*. In most of the examined regions, i.e., middle frontal, inferior frontal, parietal, temporal and primary visual cortices, advanced age was associated with smaller volume and thinner cortex at baseline. Longitudinal shrinkage was observed in frontal, parietal, anterior cingulate, and temporal cortices, but not in primary visual cortex. However, no relationship was found between cortical shrinkage and cognitive decline.

Longitudinal decline in Gf.

By modeling practice effects in the current study, we separated improvement due to practice and age-related longitudinal decline in cognitive skills. Notably, we observed a practice effect for G*f* that was 2.5 times the annual longitudinal decline, or 3.8 times the annual cross-sectional age difference. The results are consistent with previous reports in fluid intelligence that practice effects can persist for several years (Rabbitt, et al., 2004; Salthouse, et al., 2004). Salthouse and colleagues (2004) demonstrated that the practice effects on reasoning ability could persist for more than 9 years, and the magnitude of re-test gain was 17 times greater than the annual cross-sectional age-related variance (Salthouse, et al., 2004). The ratio of re-test improvement to annual cross-sectional age difference was lower in the current study than in

Salthouse's findings. Such a discrepancy might result from several reasons. First, practice gains are smaller with increased age (Salthouse, et al., 2004), and our subjects were older than their subjects. Therefore, the participants in the current study might benefit less from practice gains. Second, in the current study, the magnitude of the practice effects was computed from data from all four waves, assuming the amount of practice gain was linearly additive, i.e., the benefit from exposure to three previous test sessions was assumed to equal three times the benefit of one previous test session. However, this assumption was not verified. Thus, the practice effect could be underestimated if the gain from three previous test sessions was actually smaller than three times the benefit of one previous exposure to a test. Nevertheless, by taking practice effect into account, we were able to more precisely estimate the age-related longitudinal decline. These gains, if not estimated, could lead to underestimation or even failure to identify the true longitudinal decline (Ferrer, et al., 2005; Rabbitt, et al., 2001).

Significant longitudinal decline in G*f*, as well as significantly negative age differences in the baseline level of G*f*, are consistent with age-related decline of G*f* in middle-aged and older adults, described in the extant literature (e.g., Desjardins & Warnke, 2012; Horn & Blankson, 2005; Horn & Cattell, 1967; McArdle, et al., 2002). Interestingly, in our sample, the rate of decline in G*f* is accelerated by advancing age. We further found that the age-related acceleration of G*f* decline is associated with age-related slowing. This conclusion is based on two analyses: First, the acceleration of longitudinal decline, which was originally observed in timed G*f* scores, was not significant for untimed G*f*. Having sufficient time seems to equalize the individual rates of decline, while preserving the magnitude of mean change. Second, when the processing speed was controlled, the longitudinal decline in timed G*f* did not accelerate with age. Thus age-related

slowing is an important factor contributing to the acceleration of G*f* decline. In the current study, processing speed was measured by letter comparison and pattern comparison, both of which require aspects of processing speed that are necessary for completing CFIT. The tests included in the CFIT task require participants to read the problem, compare the designs, and search for the correct items to match. Therefore, not surprisingly, faster processing speed was related to better timed G*f* at baseline, but it was not related to untimed G*f*.

Longitudinal shrinkage of cortices.

In our sample, cortices of healthy participants underwent significant shrinkage. We observed shrinkage of the prefrontal, parietal, anterior cingulate, and temporal cortices, and relative stability of the primary visual cortex. The differential change across cortical regions was consistent with previous reports that association (prefrontal and parietal) cortices were more vulnerable to aging than the occipital region (Raz, et al., 2010; Raz, et al., 2005; Resnick, et al., 2003). In addition, in cross-sectional studies, greater age differences have been demonstrated in prefrontal and parietal cortices (Fjell, Westlye, et al., 2009; Raz, et al., 1997; Salat, et al., 2004). The results of the current study replicated a number of previous findings (Driscoll, et al., 2009; Fjell, Walhovd, et al., 2009; Fjell, Westlye, et al., 2009; Raz, et al., 2010; Raz, et al., 2005). However, some previous findings were not replicated, such as the accelerated shrinkage of frontal and parietal cortices (Driscoll, et al., 2009). This discrepancy might result from two reasons. First, our participants were younger than Driscoll's subjects (63.81 ± 9.08 years in our sample vs. 70.58 ± 6.11 in Driscoll's normal sample). It is possible that the accelerated decline is more noticeable in the oldest old. The second possible reason is the difference in the method used to identify accelerated atrophy. In the current study, we modeled the latent growth curves and estimated

intercept (baseline) and slope of change (i.e., the changes in cortical measures were assumed to be linear for each individual participants, and accelerated shrinkage was defined by the age effect on individuals' slope of change). However, Driscoll's study employed linear mixed models, and included age^2 in their model, which indicated the accelerated atrophy. Thus, both linear and quadratic components of individual change were modeled. We also tried including the quadratic slopes in LGC models of cortical change. However, as presented in table 10, negative quadratic slope was not found in prefrontal or parietal cortices, thus acceleration of shrinkage was not supported. Driscoll's study had scans of up to 10 waves, sufficient to describe linear and non-linear change. However, in the current 4-wave study, we had only 18 participants with MRI scans of all 4 waves. Small sample size and substantial missing data might lead to non-significance of the quadratic slope factor.

Another discrepancy with previous findings involves the presence of individual differences in shrinkage rate. In the current study, the shrinkage rate variance was not significant in any of the investigated regions. However, in a previous study (Raz, et al., 2010), in which the measures and subjects overlapped to a large extent with the current project, individual differences in shrinkage rates were significantly related to volumes of lateral prefrontal cortex. In that study, the shrinkage rates were estimated from two consecutive waves (wave 1 and wave 2, or wave 2 and wave 3), while in the current study, shrinkage rates were calculated across all the 4 waves. Thus, while the individual differences in prefrontal cortex shrinkage rates were significant in one study but were not significant in the other study, the results from two studies did not necessarily conflict with each other, because they employed shrinkage measures that were defined differently. Nevertheless, when we model latent difference using similar method,

individual variances in the change of cortical thickness and volume were significant in middle frontal cortex, as presented in table 11.

For MF in the current study, a significant rate of shrinkage was observed for atrophy, but not for cortical thickness. Age-related shrinkage in cortical volume was not equivalent to shrinkage in cortical thickness. In contrast, the reduction of surface area was significant in all cortical regions examined. Because cortical volume could be seen as the product of cortical thickness and surface area, the results suggested that the age-related reduction of cortical volume combines cortical thinning and shrinkage in surface area. Correlation ranges for volume-thickness ranged between r = 0.151 and 0.601; for volume-area: [0.276, 0.697]. Median values of r were 0.23, 0.40, 0.49, 0.38, 0.21, 0.58 for the volume-thickness of IF, MF, PC, VC, ACC, TC, respectively; and 0.57, 0.48, 0.41, 0.66, 0.68, 0.34 for the volume-area of IF, MF, PC, VC, ACC, TC, respectively. Median r's in each wave were 0.37, 0.37, 0.46, 0.40 for volume-thickness and 0.51, 0.54, 0.50, 0.47 for volume-area.

Relationship between changes in Gf and cortices.

We hypothesized positive associations between G*f* and cortical size at baseline, and between the change rates of cortices and G*f*. However, no such relationship was found between the parameters of G*f* change and parameters of cortical change. According to Jung and Haier's P-FIT, G*f* depends on the integrity of parietal and frontal regions. Nevertheless, it is possible that CFIT is not sensitive to the volume and thickness of the cortical regions investigated in the current study. Perhaps only the volume or thickness of very small regions within prefrontal and parietal cortices are related to CFIT. For example, a study using voxel-based morphometry (VBM)

reported G*f* to be correlated with the volumes of small clusters in dorsolateral prefrontal cortex (Colom, et al., 2009). The clusters included some sub-regions within middle and inferior frontal gyri, but not the entire MF and IF, and it is unclear if the observed associations would remain after mapping the function on anatomically defined regions rather than arbitrary units like voxels. Previous studies have also suggested that using neuroanatomically-defined voxel clusters based on automated techniques produces results that may differ from manually traced regions. However, this discrepancy disappears once the realistic anatomical boundaries are drawn (Kennedy, et al., 2009). The ROI method employed in the current study is a straightforward approach for estimating relationships with behavior in selected target regions that are based on their neuroanatomical properties and previously demonstrated associations with the tested indices of cognition. If the cortex-behavior correlation is uniform over the ROI, then the association may be highlighted by averaging across the whole ROI. On the other hand, when there is random correlation between cognition and cortical size in one part of the ROI, it can be averaged out using the uncorrelated regions or regions with correlations in the opposite direction. Thus, spurious findings due to random noise can be diminished.

Limitations of the current study.

The current study has some limitations. First, in modeling the LGC of G*f* change, re-test effect was simply interpreted in term of number of previous assessment. In fact, several factors might influence the magnitude of practice effects (e.g., time interval from last assessment (Salthouse, et al., 2004), and interaction between time intervals and numbers of previous assessment). Longitudinal measures with varying time intervals between measures would be needed to address this complex issue. Second, small sample size in the current study could limit

the power of analyses. It is possible that some marginally significant effects would become significant when the sample size gets larger.

Conclusion.

In summary, the current longitudinal study modeled age-related change in fluid intelligence, crystallized intelligence, processing speed, as well as the longitudinal shrinkage in prefrontal, parietal, anterior cingulate, temporal and primary visual cortex. Longitudinal decline was observed in G*f* and was accelerated by older age. By referring to the LGCs of processing speed and untimed CFIT, we proposed that the acceleration of G*f* decline could be at least partly explained by age-related slowing of processing speed. Intra-person longitudinal shrinkage was observed for cortical thickness and volume of prefrontal, parietal, anterior cingulate, and temporal cortices, but not in primary visual cortex. However, reduction of cortical surface area was observed in all the examined regions, including primary visual cortex. No association was found between the parameters of cognitive change and parameters of cortical change.

TABLES

Table 1. Descriptive statistics of longitudinal measures.

	Interval from baseline (month)			N	age (year)		
	mean	sd	range		mean	sd	range
baseline	0	--	--	46	63.81	9.08	49.50 - 83.33
1st follow-up	16.0	1.7	13 - 23	40	65.45	9.28	50.75 - 84.67
2nd follow-up	31.3	2.9	27 - 39	31	66.59	9.43	52.17 - 85.67
3rd follow-up	90.2	6.0	81 - 102	27	71.02	9.10	57.17 - 91.17

Table 2. Fit indices of CFA models on prefrontal cortical thickness.

	Model a basic regions	Model b Basic + frontal pole & superior frontal	Model c Basic + superior frontal	Model d Basic + frontal pole	Model e Split PFC into middle & inferior frontal
χ^2	61.549	153.273	96.879	96.538	48.024
df	35	77	54	54	34
p-Value	0.004	<0.001	<0.001	<0.001	0.056
χ^2/df	1.758	1.990	1.794	1.787	1.412
AIC	1150.204	1545.991	1321.173	1363.600	1138.679
BIC	1203.730	1620.927	1385.404	1427.831	1193.989
RMSEA	0.131	0.150	0.134	0.134	0.097
CFI	0.828	0.761	0.832	0.800	0.909
SRMR	0.084	0.091	0.086	0.091	0.082

Table 3. Fit indices of CFA models on prefrontal cortical volume.

	Model a basic regions	Model b Basic + frontal pole & superior frontal	Model c Basic + superior frontal	Model d Basic + frontal pole	Model e Split PFC into middle & inferior frontal
χ^2	82.258	139.114	112.282	105.217	66.049
df	35	77	54	54	34
p-Value	<0.001	<0.001	<0.001	<0.001	0.001
χ^2/df	2.350	1.807	2.079	1.948	1.943
AIC	1118.047	1518.945	1278.714	1360.889	1103.838
BIC	1171.572	1593.881	1342.945	1425.119	1159.148
RMSEA	0.175	0.135	0.157	0.147	0.146
CFI	0.772	0.813	0.814	0.772	0.845
SRMR	0.091	0.086	0.084	0.091	0.082

Table 4. Fit indices of CFA models on parietal cortical thickness.

	Model a Basic regions	Model b Basic + precuneus
χ2	5.721	21.041
df	6	16
p-Value	0.455	0.177
χ2/df	0.954	1.315
AIC	642.848	843.879
BIC	680.316	893.836
RMSEA	0.000	0.085
CFI	1.000	0.973
SRMR	0.025	0.041

Table 5. Fit indices of CFA models on parietal cortex volume.

	Model a Basic regions	Model b Basic + precuneus
χ2	29.158	48.437
Df	6	16
p-Value	0.0001	0.000
χ2/df	4.860	3.027
AIC	615.987	769.991
BIC	653.455	819.949
RMSEA	0.296	0.215
CFI	0.869	0.888
SRMR	0.042	0.058

Table 6. Fit indices of measurement models of cortical measures.

	cortical thickness		surface area		volume	
	6-factor	1 factor	6-factor	1 factor	6-factor	1 factor
χ2	70.080	91.265	58.397	81.724	75.789	99.371
df	45	59	45	59	49	59
p-Value	0.010	0.005	0.087	0.027	0.008	0.001
χ2/df	1.557	1.547	1.298	1.385	1.547	1.684
AIC	1221.471	1214.656	999.438	994.765	1117.692	1121.275
BIC	1323.170	1291.376	1101.137	1071.485	1212.254	1197.995
RMSEA	0.113	0.111	0.082	0.094	0.111	0.125
CFI	0.932	0.913	0.977	0.961	0.910	0.864
SRMR	0.049	0.072	0.030	0.052	0.076	0.101

Table 7. Results of LGC models on ROI volumes.

ROI	age difference in baseline volume				age differences in slope		slope of change				residual variance of slope	
	mean	*p*	95% CI		mean	*p*	mean	*p*	95% CI		mean	*p*
MF	-0.370	0.018	-0.676	-0.064	0.046	0.662	-0.783	<0.001	-0.965	-0.601	0.054	0.417
IF	-0.373	0.006	-0.638	-0.108	0.034	0.718	-0.738	<0.001	-0.907	-0.569	0.093	0.100
PC	-0.417	0.005	-0.707	-0.127	-0.088	0.310	-0.770	<0.001	-0.954	-0.586	0.090	0.102
ACC	-0.030	0.825	-0.312	0.252	0.008	0.930	-0.203	0.002	-0.328	-0.078	0.022	0.492
TC	-0.279	0.175	-0.683	0.125	-0.255	0.089	-0.805	<0.001	-1.023	-0.587	0.115	0.310
VC	-0.519	<0.001	-0.786	-0.252	-0.011	0.916	-0.061	0.537	-0.255	0.133	0.086	0.423

Table 8. Results of LGC models on ROI thickness.

ROI	age effect on baseline thickness				age effect on slope		slope of change				residual variance of slope	
	mean	*p*	95% CI		mean	*p*	mean	*p*	95% CI		mean	*p*
MF	-0.405	0.008	-0.705	-0.105	0.203	0.419	-0.125	0.499	-0.488	0.238	0.194	0.564
IF	-0.195	<0.001	-0.262	-0.128	0.035	0.178	-0.233	<0.001	-0.284	-0.182	0.014	0.449
PC	-0.511	<0.001	-0.756	-0.266	-0.127	0.259	-0.551	<0.001	-0.784	-0.318	0.016	0.848
ACC	-0.010	0.953	-0.351	0.331	0.163	0.346	-0.155	0.250	-0.420	0.110	0.124	0.625
TC	-0.537	<0.001	-0.780	-0.294	-0.127	0.383	-0.740	<0.001	-0.999	-0.481	0.106	0.537
VC	-0.561	<0.001	-0.820	-0.302	0.061	0.659	0.324	0.013	0.069	0.579	0.188	0.273

Table 9. Correlations between change parameters of timed CFIT, vocabulary scores, processing speed, and regional volume/thickness.

	Correlation with G*f*		Correlation with G*c*		Correlation with speed	
	intercept	slope	intercept	slope	intercept	slope
MF volume	-0.089	0.067	0.015	0.016	-0.074	0.000
IF volume	-0.097	0.108	-0.003	0.002	-0.032	0.019
PC volume	-0.038	0.059	0.066	-0.002	0.077	0.010
ACC volume	-0.017	0.026	0.049	0.002	0.065	0.001
TC volume	-0.102	0.083	0.046	-0.007	-0.048	0.019
VC volume	0.102	-0.036	0.004	0.031	0.017	-0.010
MF thickness	-0.069	0.056	-0.036	0.071	0.035	0.009
IF thickness	-0.053	0.035	-0.046	-0.004	-0.062	0.019
PC thickness	0.000	-0.011	0.005	0.019	0.092	-0.044
ACC thickness	0.016	0.095	-0.107	0.072	-0.044	-0.013
TC thickness	-0.001	0.007	0.009	0.041	0.007	0.003
VC thickness	0.004	0.000	0.011	0.048	-0.036	0.003

All $p > 0.05$.

Table 10. Results of LGC models including quadratic slope factor.

ROI	Age effect on baseline		Linear slope		Quadratic slope	
	mean	*p*	mean	*p*	mean	*p*
MF volume	-0.422	0.002	-0.764	0.001	-0.025	0.940
IF volume	-0.367	0.005	-0.677	0.011	-0.098	0.790
PC volume	-0.428	0.003	-1.327	<0.001	0.782	0.014
ACC volume	-0.032	0.822	0.255	0.217	-0.599	0.036
TC volume	-0.294	0.069	-0.418	0.203	-0.527	0.244
VC volume	-0.174	0.094	-0.533	0.014	0.506	0.053
MF thickness	-0.400	0.002	0.361	0.409	-0.579	0.276
IF thickness	-0.189	0.043	-0.130	0.660	-0.140	0.700
PC thickness	-0.540	<0.001	-0.266	0.469	-0.342	0.446
ACC thickness	0.008	0.877	0.041	0.784	-0.145	0.436
TC thickness	-0.520	<0.001	-0.907	0.019	0.245	0.627
VC thickness	-0.545	<0.001	0.888	0.007	-0.799	0.057

Table 11. Latent difference in regional volume and cortical thickness.

ROI		change in regional volume				variances of volume change		change in cortical thickness				variances of thickness change	
		mean	*p*	95% CI		Est.	*p*	mean	*p*	95% CI		Est.	*p*
MF	LD12	-0.157	0.001	-0.247	-0.067	0.053	0.004	-0.144	0.133	-0.332	0.044	0.311	<.001
	LD23	-0.042	0.442	-0.148	0.064	0.065	0.006	0.198	0.011	0.045	0.351	0.122	0.012
	LD34	-0.421	<.001	-0.558	-0.284	0.076	0.019	-0.208	0.073	-0.435	0.019	0.231	0.020
IF	LD12	-0.117	0.005	-0.197	-0.037	0.031	0.062	-0.116	0.126	-0.265	0.033	0.105	0.090
	LD23	-0.084	0.023	-0.157	-0.011	0.011	0.386	0.142	0.071	-0.013	0.297	0.056	0.261
	LD34	-0.392	<.001	-0.510	-0.274	0.040	0.088	-0.351	<.001	-0.549	-0.153	0.039	0.551
PC	LD12	-0.181	<.001	-0.277	-0.085	0.082	<.001	-0.108	0.138	-0.251	0.035	0.156	0.002
	LD23	-0.143	0.005	-0.241	-0.045	0.073	0.004	0.020	0.805	-0.141	0.181	0.170	0.010
	LD34	-0.312	<.001	-0.455	-0.169	0.083	0.005	-0.359	<.001	-0.522	-0.196	0.067	0.063
AC	LD12	0.015	0.514	-0.032	0.062	0.016	0.005	0.005	0.751	-0.022	0.032	0.019	0.578
	LD23	0.052	0.132	-0.017	0.121	0.034	0.002	-0.011	0.666	-0.060	0.038	0.024	0.652
	LD34	-0.146	0.011	-0.258	-0.034	0.040	0.023	-0.012	0.712	-0.075	0.051	0.018	0.574
TC	LD12	-0.116	0.054	-0.234	0.002	0.102	0.002	-0.221	0.002	-0.362	-0.080	0.147	0.003
	LD23	-0.010	0.899	-0.161	0.141	0.149	0.001	0.016	0.858	-0.155	0.187	0.180	0.005
	LD34	-0.460	<.001	-0.662	-0.258	0.205	0.023	-0.364	<.001	-0.556	-0.172	0.170	0.028
VC	LD12	-0.092	0.018	-0.168	-0.016	0.033	0.024	-0.054	0.409	-0.181	0.073	0.091	0.018
	LD23	-0.037	0.302	-0.108	0.034	0.023	0.076	0.193	0.013	0.040	0.346	0.117	0.045
	LD34	-0.015	0.807	-0.137	0.107	0.101	0.020	-0.013	0.831	-0.131	0.105	0.013	0.643

LD12: latent difference between time 1 and time 2; LD23: latent difference between time 2 and time 3; LD34: latent difference between time 3 and time 4.

FIGURES

Figure 1. CFA models on prefrontal cortex.

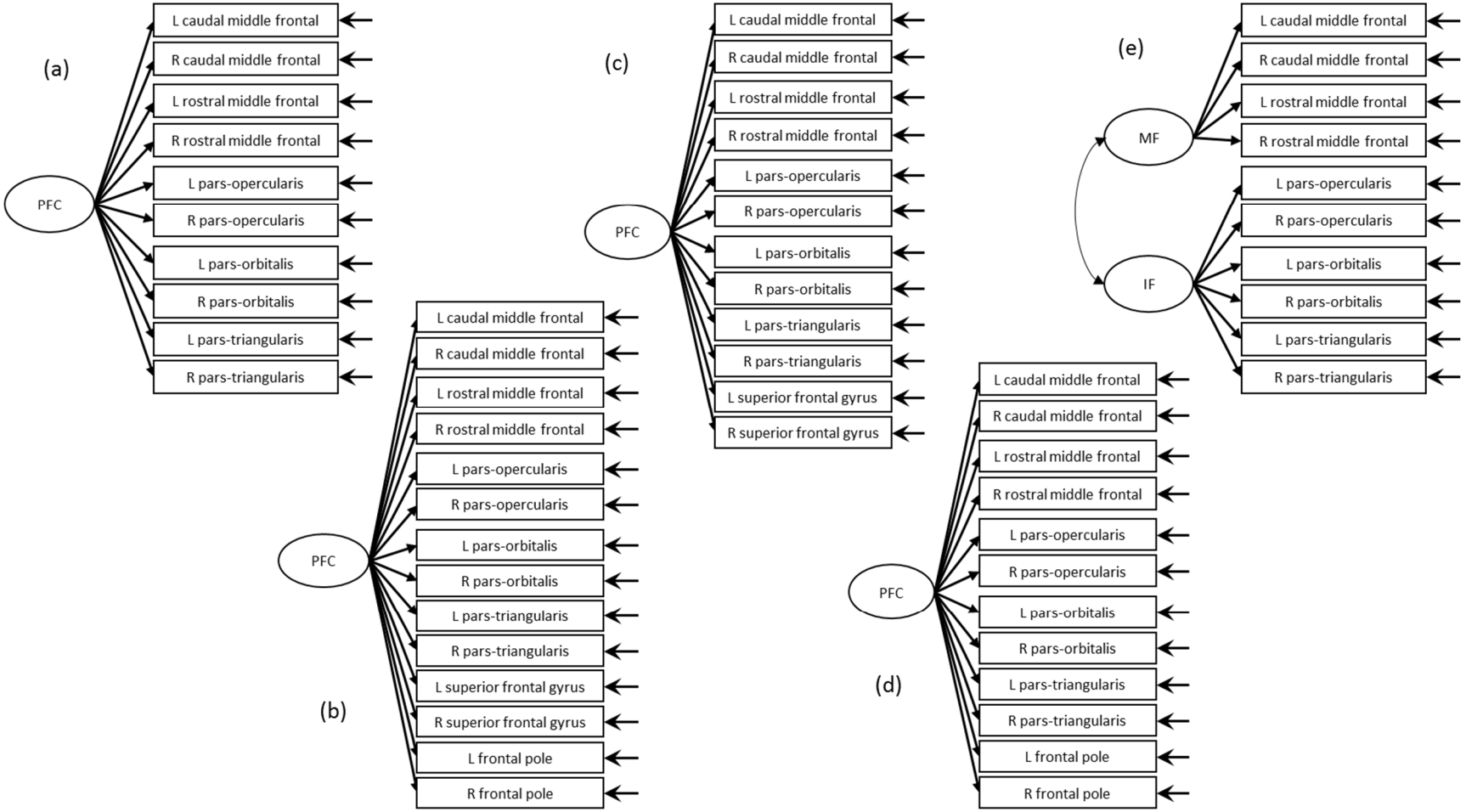

Figure 2. CFA models on parietal cortex.

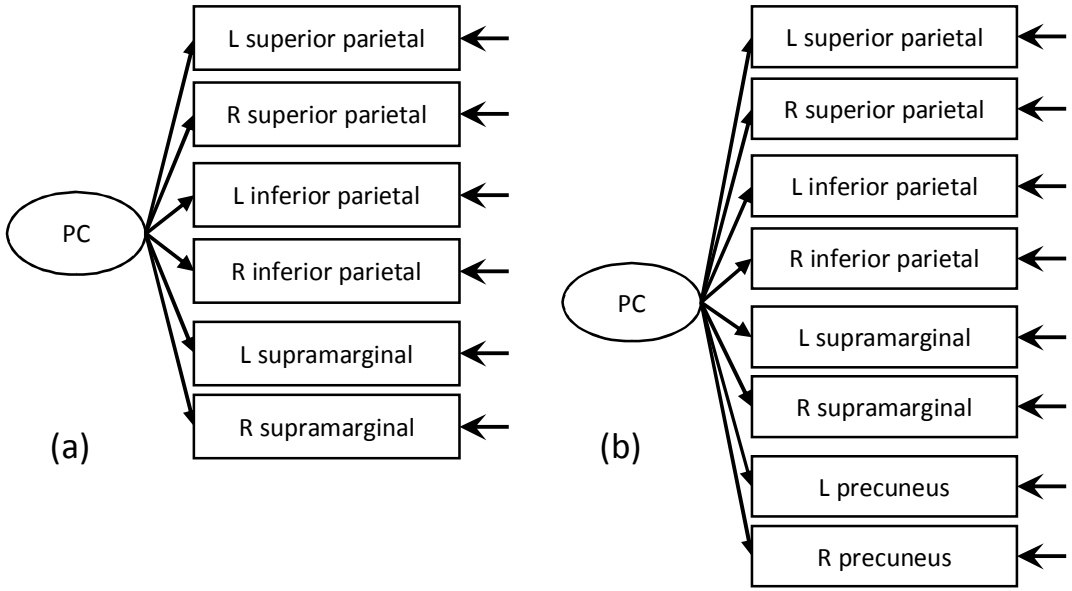

Figure 3. 6-factor vs. 1-factor measurement models.

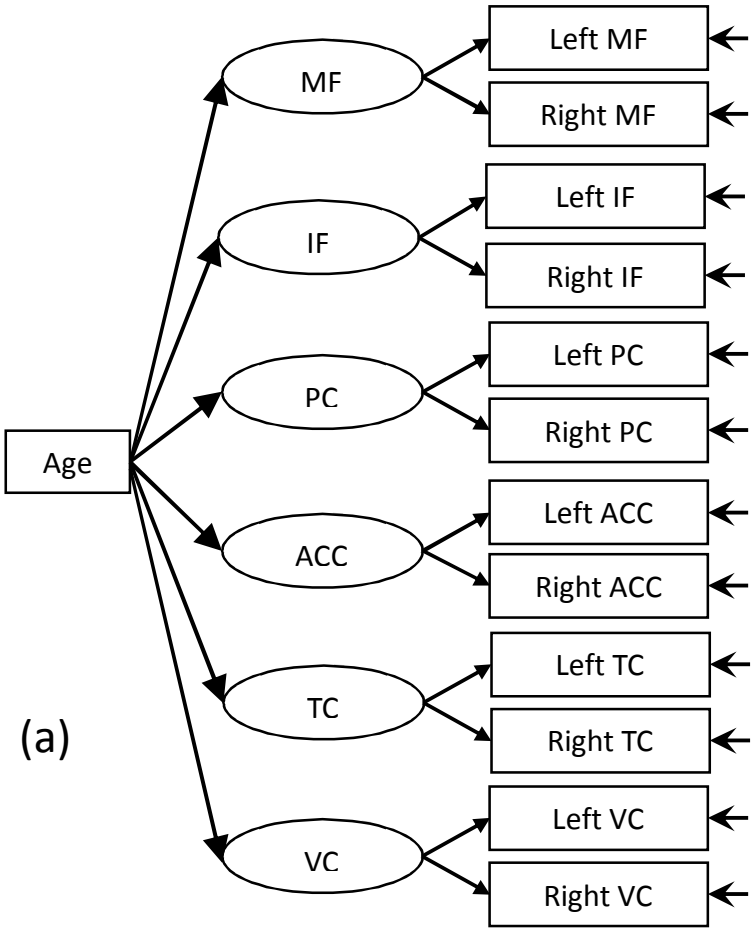

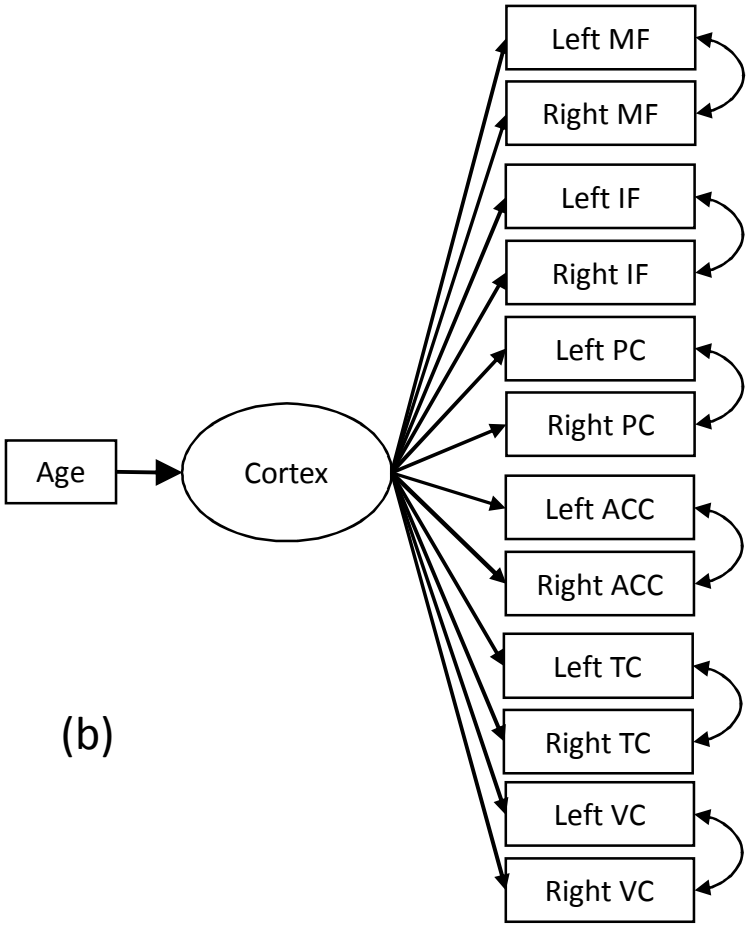

Figure 4. Latent growth curve model of G*f*.

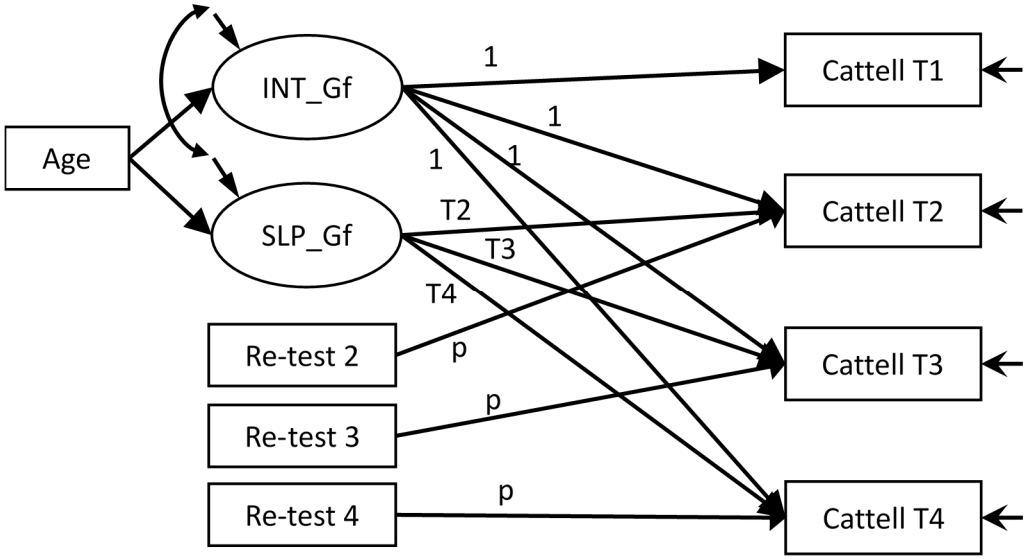

Figure 5. Latent growth curve model of G*c*.

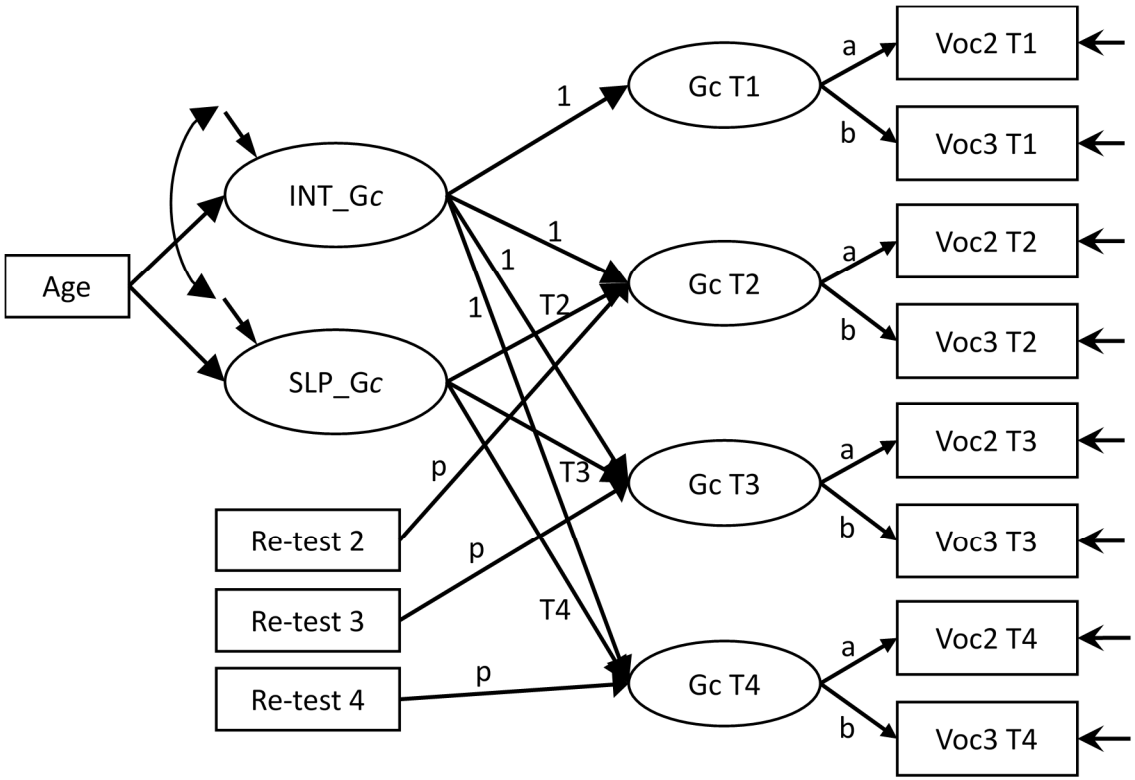

Figure 6. Latent growth curve model of ROI measures.

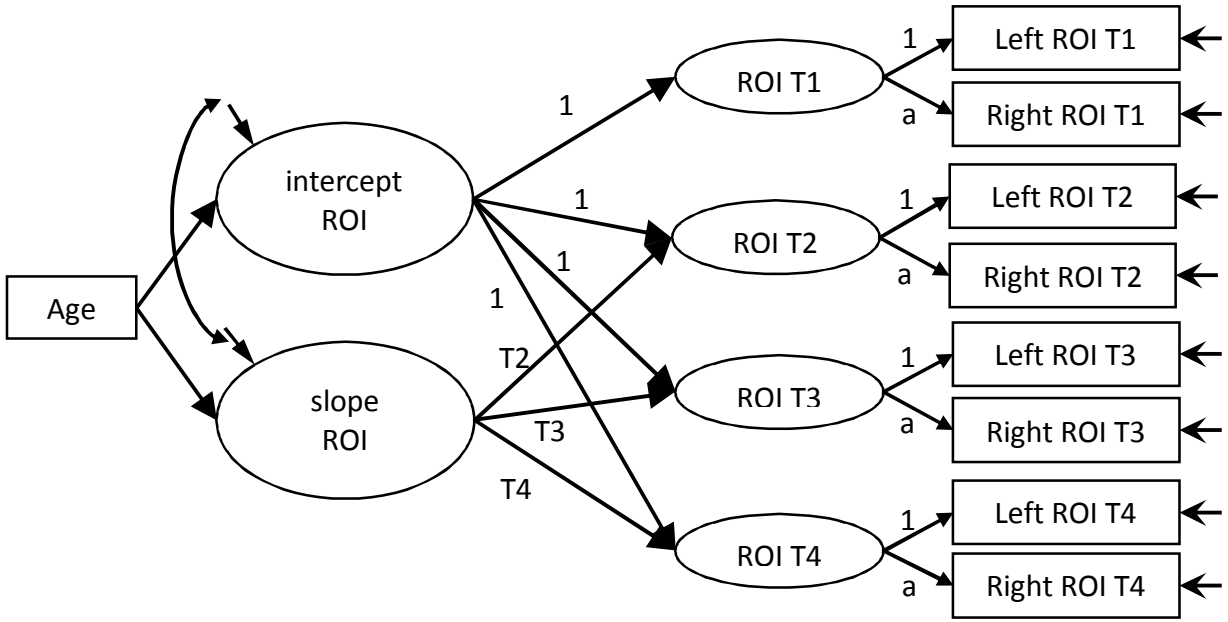

Figure 7. Longitudinal change of timed CFIT scores. Top: CFIT raw scores; bottom: CFIT scores with re-test effect controlled. Scores of the same persons were marked with same colors in two plots.

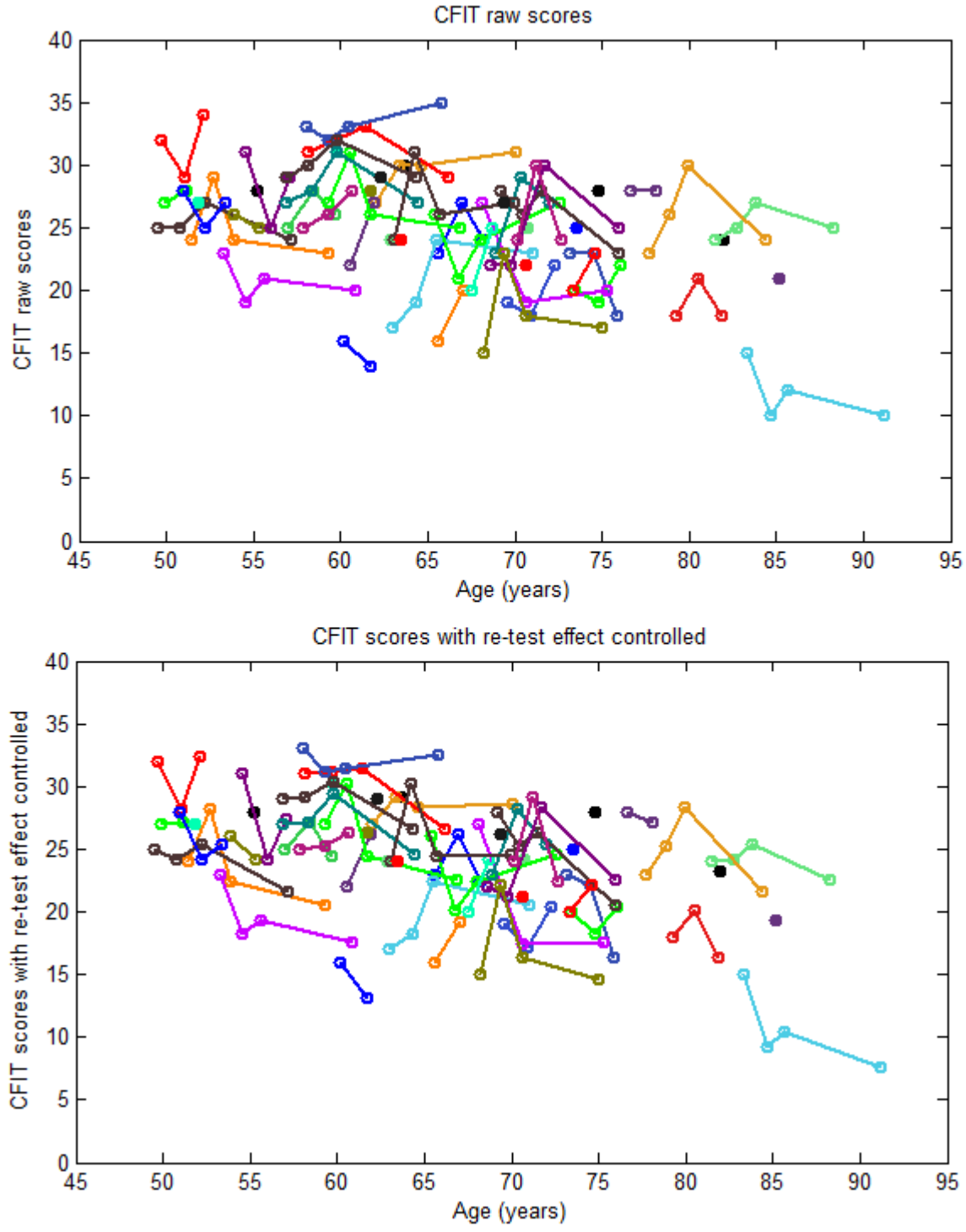

Figure 8. Longitudinal change of processing speed. Top: letter comparison; bottom: pattern comparison. Scores of the same persons were marked with same colors in two plots.

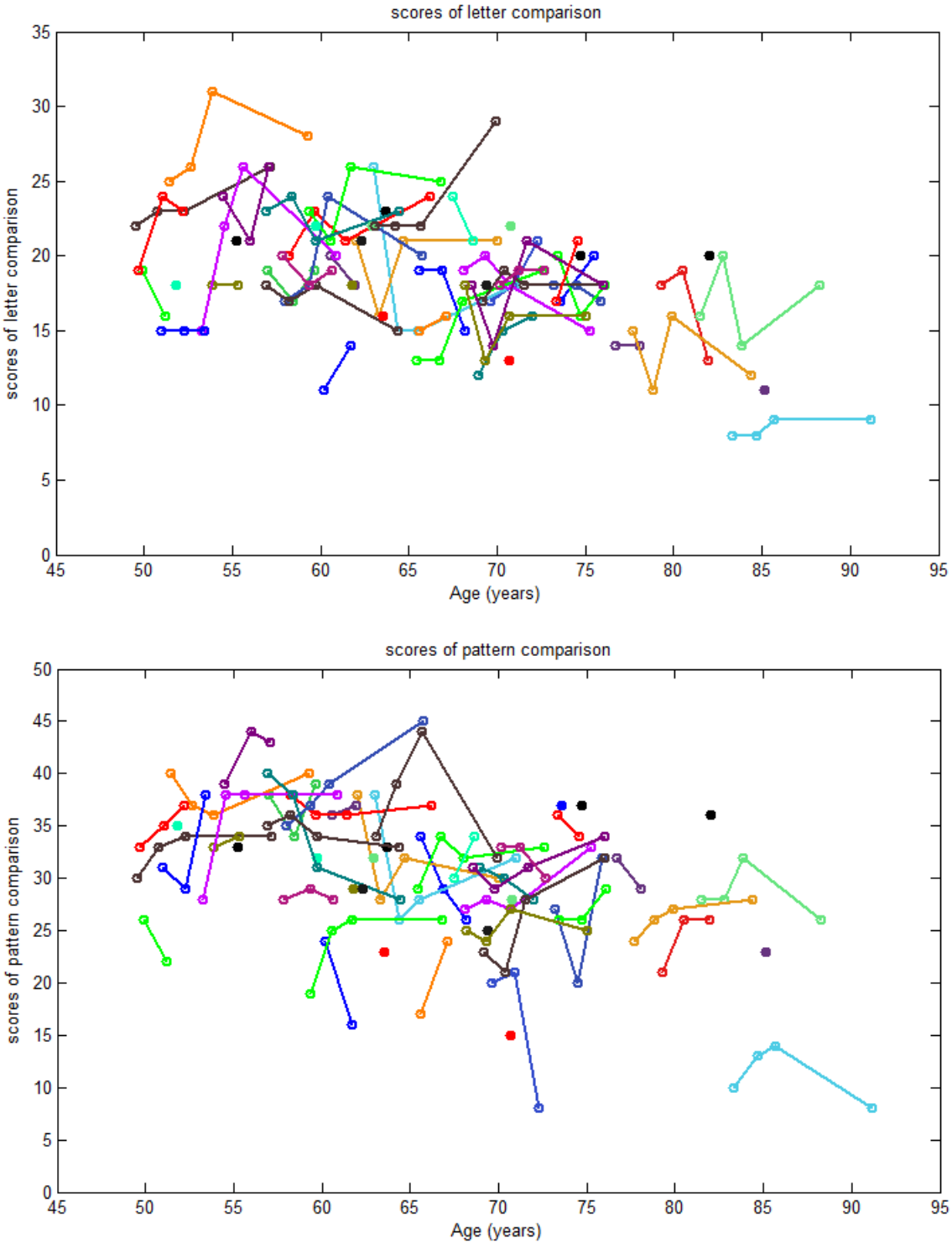

Figure 9. Longitudinal change of vocabulary scores. Top: scores of vocabulary test 2; bottom: scores of vocabulary test 3. Scores of the same persons were marked with same colors in two plots.

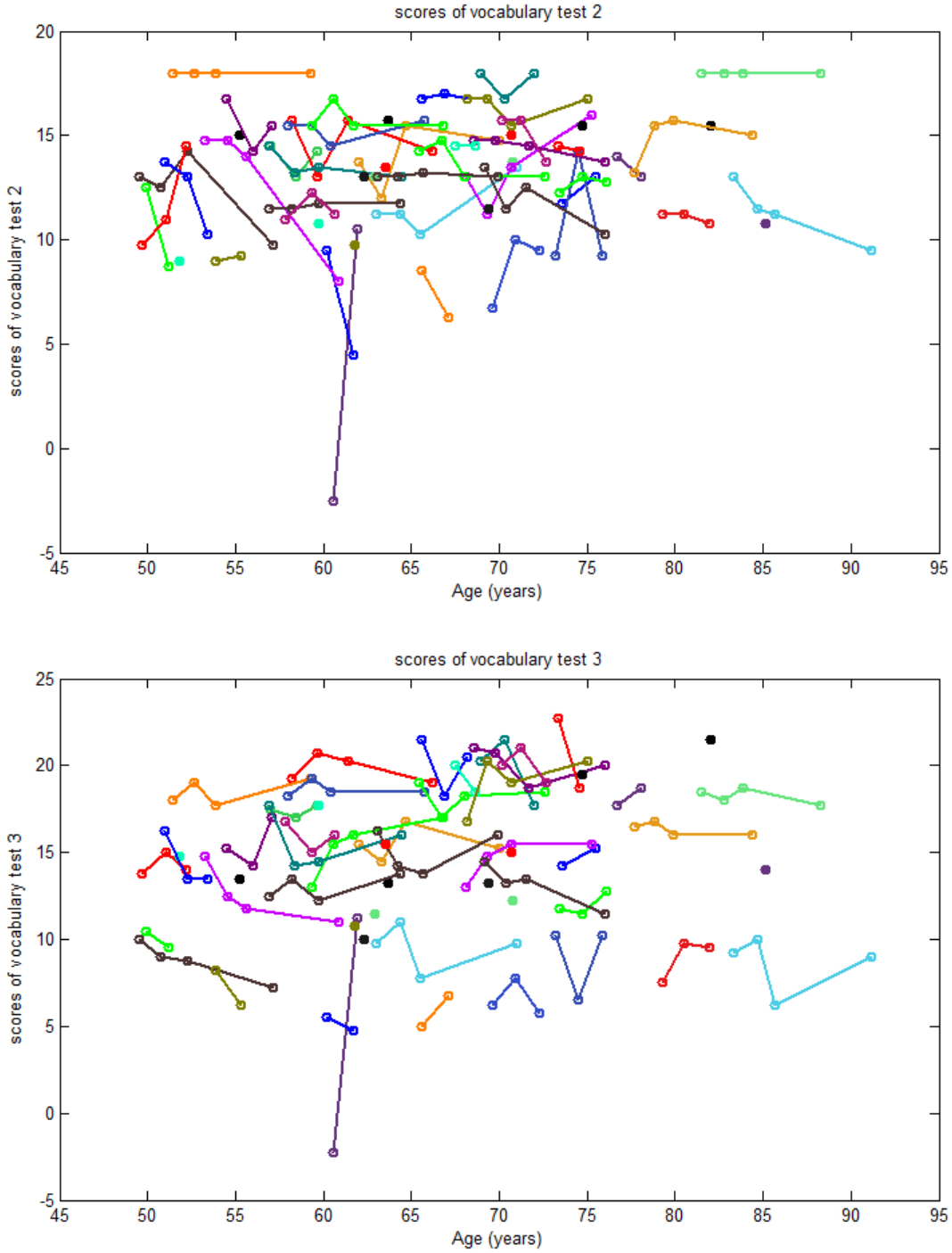

Figure 10. Combined LGC model of G*f* and G*c*.

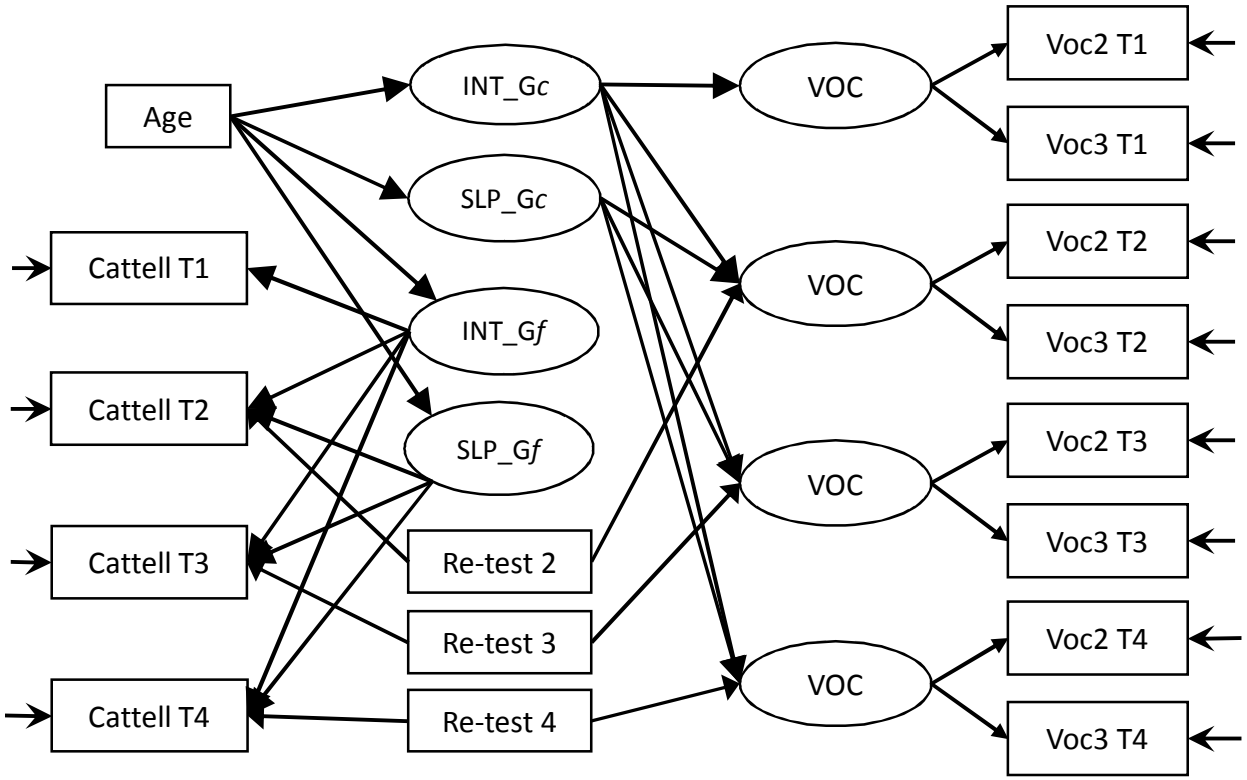

Figure 11. Longitudinal changes in cortical thickness and volume of middle frontal cortex. Volumes are adjusted for ICV.

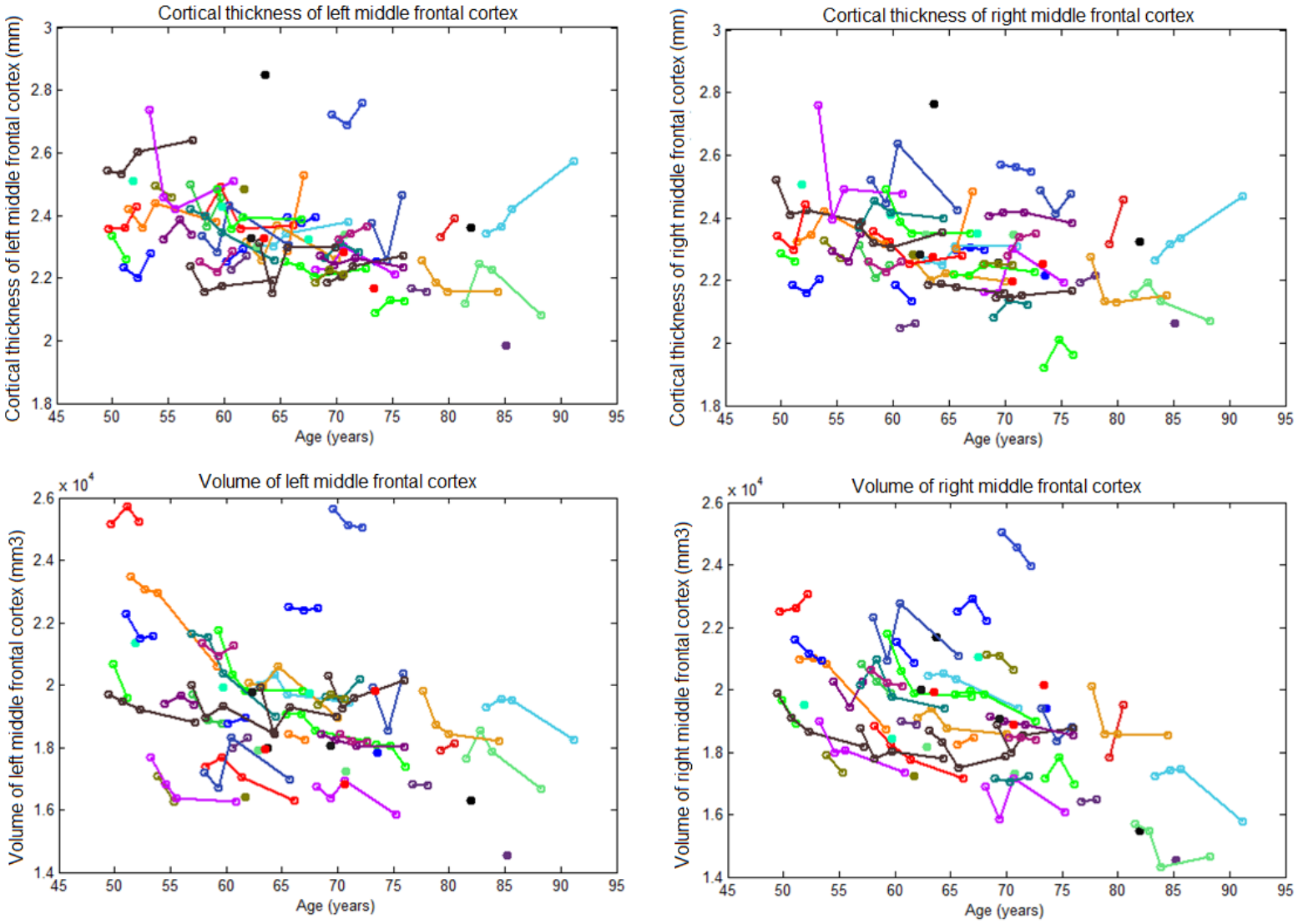

Figure 12. Longitudinal changes in cortical thickness and volume of inferior frontal cortex. Volumes are adjusted for ICV.

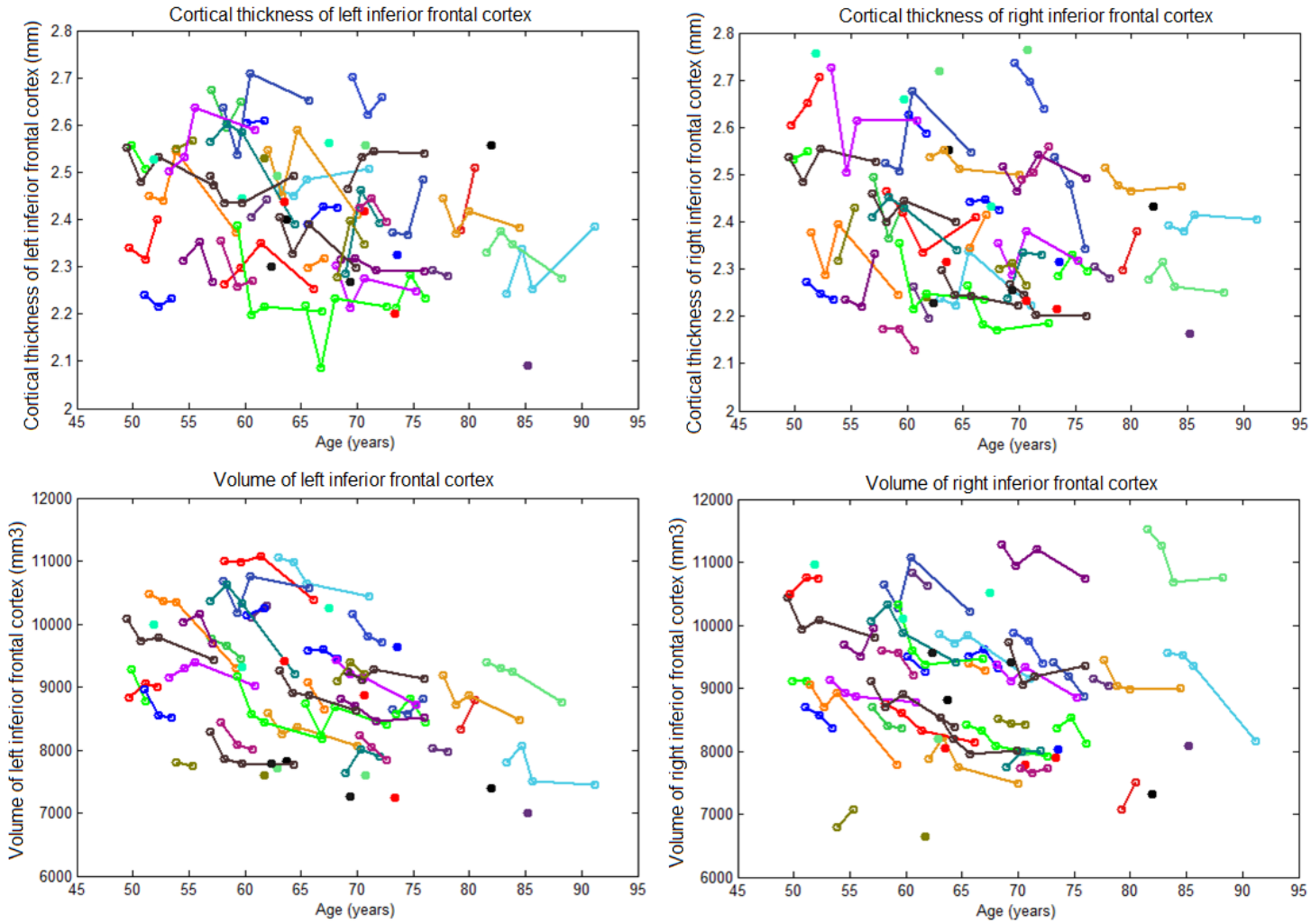

Figure 13. Longitudinal changes in cortical thickness and volume of parietal cortex. Volumes are adjusted for ICV.

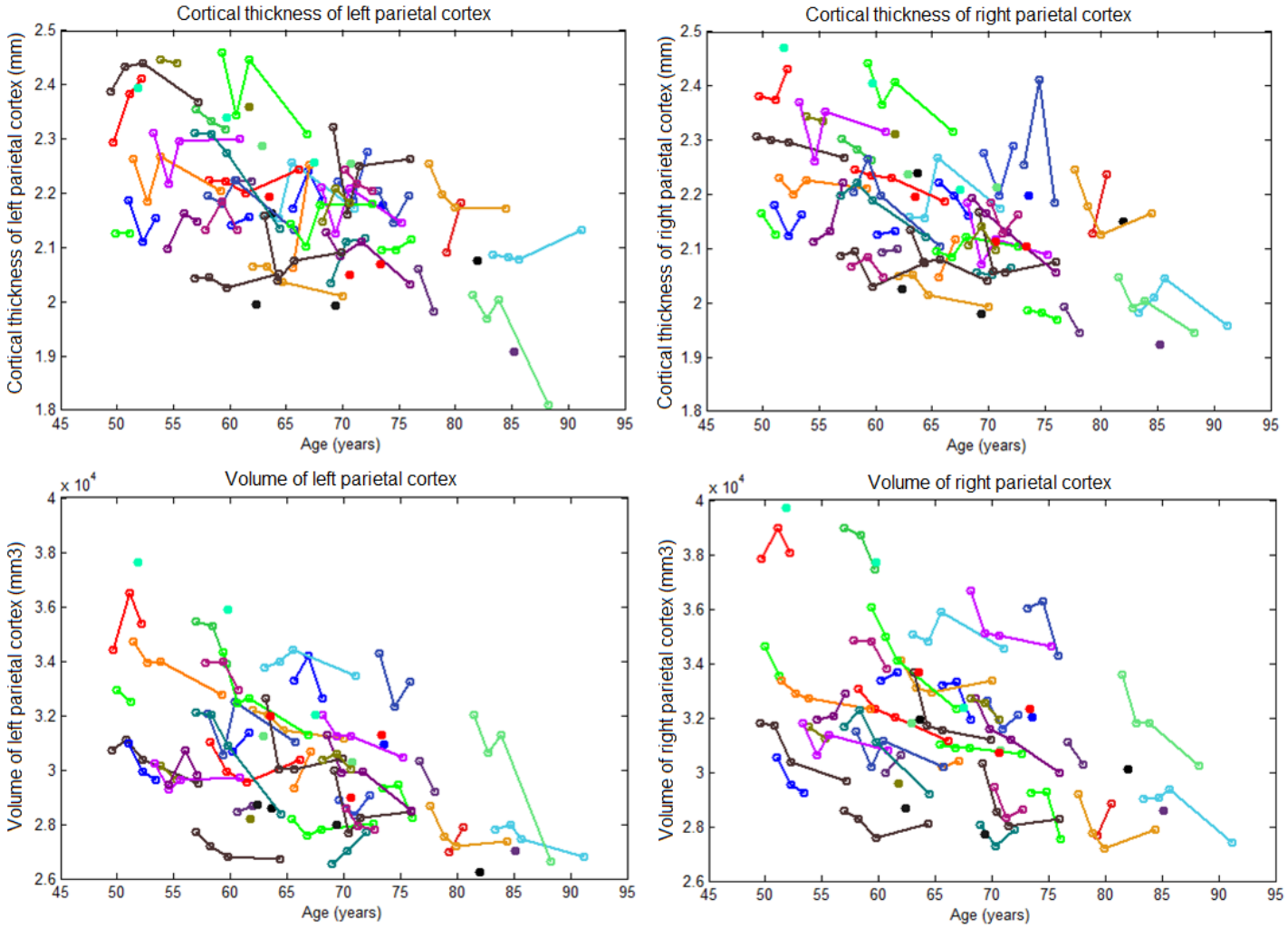

Figure 14. Longitudinal changes in cortical thickness and volume of anterior cingulate cortex. Volumes are adjusted for ICV.

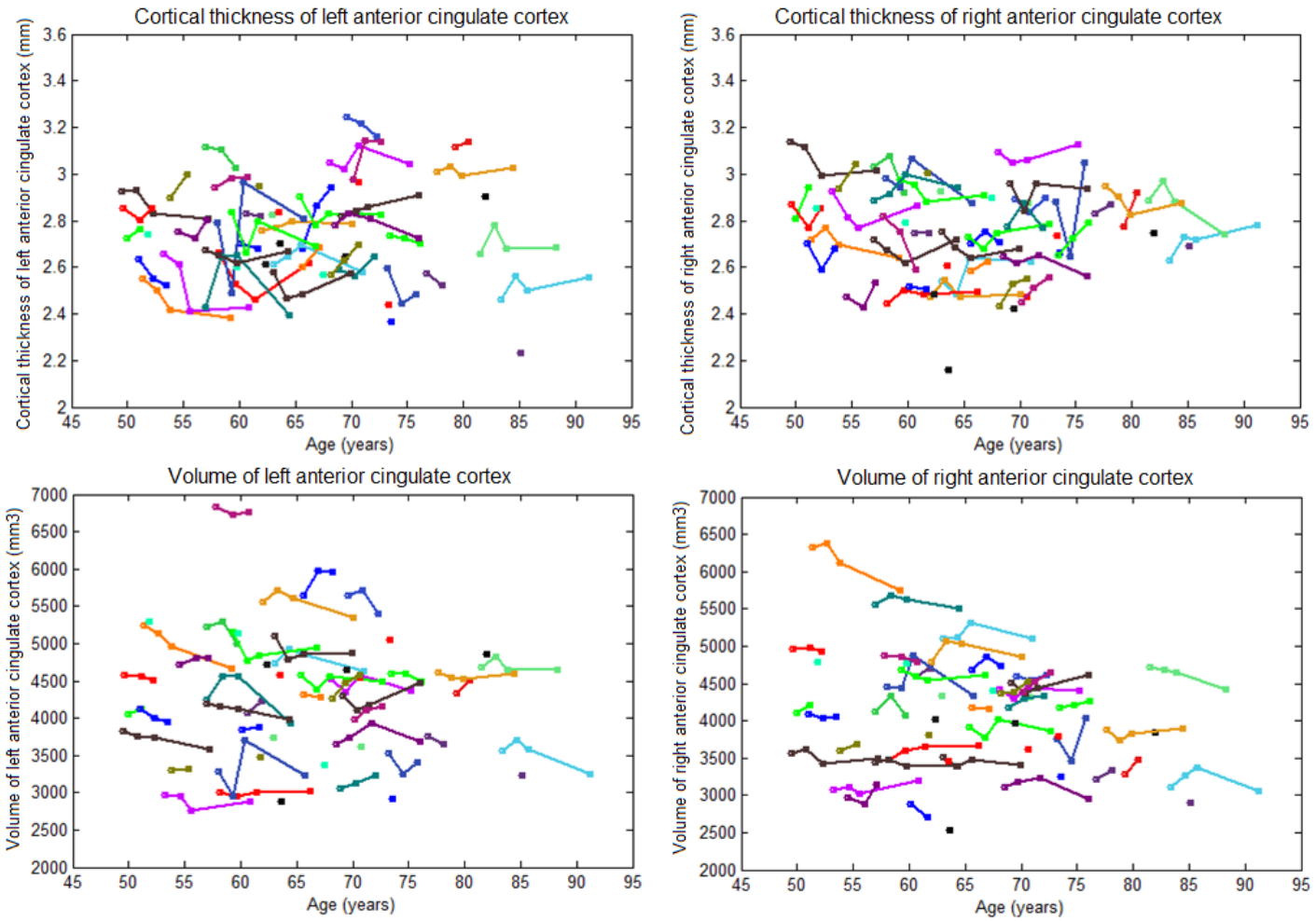

Figure 15. Longitudinal changes in cortical thickness and volume of temporal cortex. Volumes are adjusted for ICV.

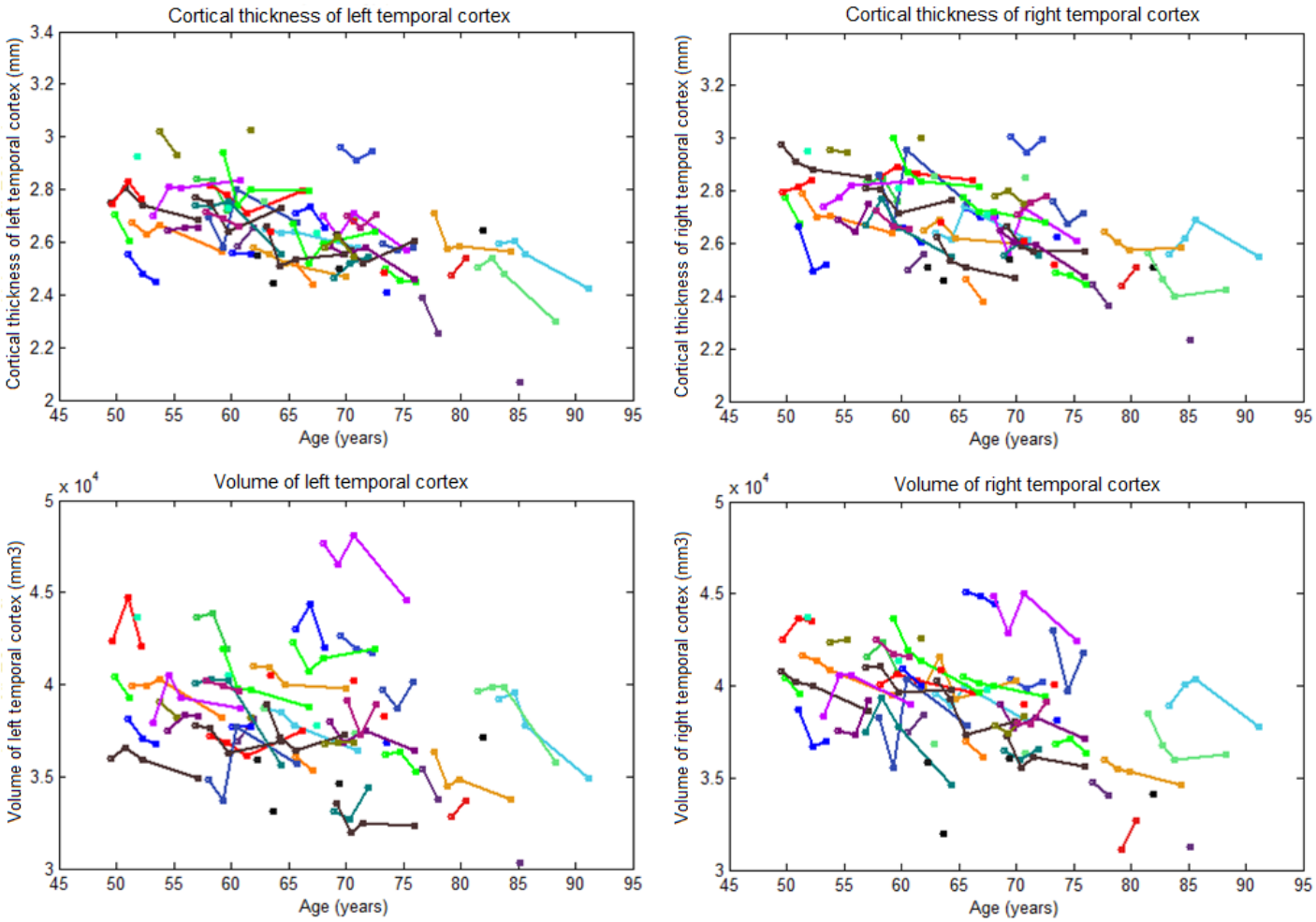

Figure 16. Longitudinal changes in cortical thickness and volume of primary visual cortex. Volumes are adjusted for ICV.

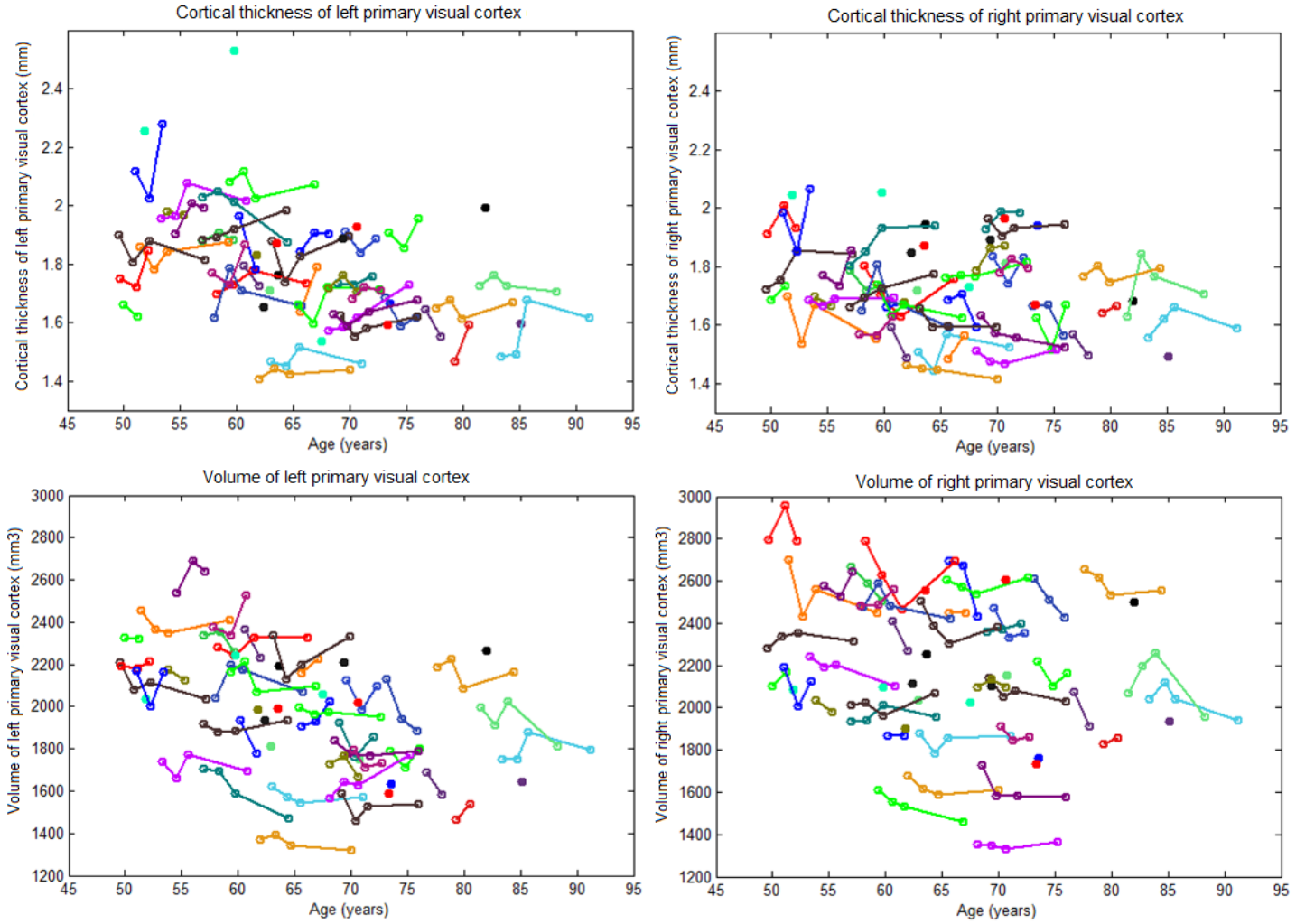

REFERENCES

Blair, C. (2006). How similar are fluid cognition and general intelligence? A developmental neuroscience perspective on fluid cognition as an aspect of human cognitive ability. *Behavioral and Brain Sciences, 29*(02), 109-125.

Braver, T. S., Barch, D. M., Gray, J. R., Molfese, D. L., & Snyder, A. (2001). Anterior cingulate cortex and response conflict: effects of frequency, inhibition and errors. *Cereb Cortex, 11*(9), 825-836.

Burgess, G. C., Braver, T. S., & Gray, J. R. (2006). Exactly how are fluid intelligence, working memory, and executive function related? Cognitive neuroscience approaches to investigating the mechanisms of fluid cognition. *Behavioral and Brain Sciences, 29*(02), 128-129.

Carroll, J. B. (1993). *Human cognitive abilities: A survey of factor-analytic studies*: Cambridge University Press.

Cattell, R. B. (1943). The measurement of adult intelligence. *Psychological Bulletin, 40*(3), 153-193.

Cattell, R. B. (1971). Abilities: their structure, growth, and action.

Cattell, R. B., & Cattell, A. (1973). *Measuring intelligence with the culture fair tests*. Champagne, IL: Institute for Personality and Ability Testing.

Chan, R. C., Shum, D., Toulopoulou, T., & Chen, E. Y. (2008). Assessment of executive functions: review of instruments and identification of critical issues. *Arch Clin Neuropsychol, 23*(2), 201-216.

Colom, R., Haier, R. J., Head, K., Álvarez-Linera, J., Quiroga, M. Á., Shih, P. C., et al. (2009). Gray matter correlates of fluid, crystallized, and spatial intelligence: Testing the P-FIT model. *Intelligence, 37*(2), 124-135.

Colom, R., Rebollo, I., Palacios, A., Juan-Espinosa, M., & Kyllonen, P. C. (2004). Working memory is (almost) perfectly predicted by g. *Intelligence, 32*(3), 277-296.

de Jong, P. F., & Das-Smaal, E. (1995). Attention and intelligence: The validity of the Star Counting Test. *Journal of Educational Psychology, 87*(1), 80.

Desikan, R. S., Segonne, F., Fischl, B., Quinn, B. T., Dickerson, B. C., Blacker, D., et al. (2006). An automated labeling system for subdividing the human cerebral cortex on MRI scans into gyral based regions of interest. *Neuroimage, 31*(3), 968-980.

Desjardins, R., & Warnke, A. J. (2012). *Ageing and skills: a review and analysis of skill gain and skill loss over the lifespan and over time*: OECD Education Working Papers.

Driscoll, I., Davatzikos, C., An, Y., Wu, X., Shen, D., Kraut, M., et al. (2009). Longitudinal pattern of regional brain volume change differentiates normal aging from MCI. *Neurology, 72*(22), 1906-1913.

Duncan, J., Seitz, R. J., Kolodny, J., Bor, D., Herzog, H., Ahmed, A., et al. (2000). A neural basis for general intelligence. *Science, 289*(5478), 457-460.

Ekstrom, R. B., French, J. W., Harman, H. H., & Dermen, D. (1976). Manual for kit of factor-referenced cognitive tests. *Princeton, NJ: Educational Testing Service*.

Engle, R. W., Tuholski, S. W., Laughlin, J. E., & Conway, A. R. (1999). Working memory, short-term memory, and general fluid intelligence: a latent-variable approach. *Journal of experimental psychology: General, 128*(3), 309.

Ferrer, E., Salthouse, T. A., McArdle, J. J., Stewart, W. F., & Schwartz, B. S. (2005). Multivariate modeling of age and retest in longitudinal studies of cognitive abilities. *Psychol Aging, 20*(3), 412-422.

Fischl, B., van der Kouwe, A., Destrieux, C., Halgren, E., Segonne, F., Salat, D. H., et al. (2004). Automatically parcellating the human cerebral cortex. *Cereb Cortex, 14*(1), 11-22.

Fjell, A. M., Walhovd, K. B., Fennema-Notestine, C., McEvoy, L. K., Hagler, D. J., Holland, D., et al. (2009). One-year brain atrophy evident in healthy aging. *J Neurosci, 29*(48), 15223-15231.

Fjell, A. M., Westlye, L. T., Amlien, I., Espeseth, T., Reinvang, I., Raz, N., et al. (2009). High consistency of regional cortical thinning in aging across multiple samples. *Cereb Cortex, 19*(9), 2001-2012.

Flanagan, D. P., & McGrew, K. S. (1998). Interpreting Intelligence Tests from Contemporary< i> Gf-Gc</i> Theory: Joint Confirmatory Factor Analysis of the WJ-R and KAIT in a Non-White Sample. *Journal of School Psychology, 36*(2), 151-182.

Folstein, M. F., Folstein, S. E., & McHugh, P. R. (1975). "Mini-mental state". A practical method for grading the cognitive state of patients for the clinician. *J Psychiatr Res, 12*(3), 189-198.

Garlick, D., & Sejnowski, T. J. (2006). There is more to fluid intelligence than working memory capacity and executive function. *Behavioral and Brain Sciences, 29*(02), 134-135.

Gauthier, I., Tarr, M. J., Moylan, J., Skudlarski, P., Gore, J. C., & Anderson, A. W. (2000). The fusiform "face area" is part of a network that processes faces at the individual level. *J Cogn Neurosci, 12*(3), 495-504.

Geake, J. G., & Hansen, P. C. (2005). Neural correlates of intelligence as revealed by fMRI of fluid analogies. *NeuroImage, 26*(2), 555-564.

Goel, V., & Dolan, R. J. (2004). Differential involvement of left prefrontal cortex in inductive and deductive reasoning. *Cognition, 93*(3), B109-121.

Gong, Q. Y., Sluming, V., Mayes, A., Keller, S., Barrick, T., Cezayirli, E., et al. (2005). Voxel-based morphometry and stereology provide convergent evidence of the importance of medial prefrontal cortex for fluid intelligence in healthy adults. *Neuroimage, 25*(4), 1175-1186.

Heitz, R. P., Redick, T. S., Hambrick, D. Z., Kane, M. J., Conway, A. R., & Engle, R. W. (2006). Working memory, executive function, and general fluid intelligence are not the same. *Behavioral and Brain Sciences, 29*(02), 135-136.

Hofer, S. M., & Sliwinski, M. J. (2001). Understanding ageing - An evaluation of research designs for assessing the interdependence of ageing-related changes. *Gerontology, 47*(6), 341-352.

Horn, J. L., & Blankson, N. (2005). Foundations for better understanding of cognitive abilities. In D. Flanagan & P. Harrison (Eds.), *Contemporary intellectual assessment: Theories, tests, and issues* (2 ed., pp. 41-67). New York: Guilford Press.

Horn, J. L., & Cattell, R. B. (1966). Refinement and test of the theory of fluid and crystallized general intelligences. *Journal of educational psychology, 57*(5), 253.

Horn, J. L., & Cattell, R. B. (1967). Age differences in fluid and crystallized intelligence. *Acta Psychol (Amst), 26*(2), 107-129.

Jancke, L., Wustenberg, T., Scheich, H., & Heinze, H. J. (2002). Phonetic perception and the temporal cortex. *Neuroimage, 15*(4), 733-746.

Jung, R. E., & Haier, R. J. (2007). The Parieto-Frontal Integration Theory (P-FIT) of intelligence: converging neuroimaging evidence. *Behav Brain Sci, 30*(2), 135-154; discussion 154-187.

Kennedy, K. M., Erickson, K. I., Rodrigue, K. M., Voss, M. W., Colcombe, S. J., Kramer, A. F., et al. (2009). Age-related differences in regional brain volumes: A comparison of optimized voxel-based morphometry to manual volumetry. *Neurobiology of Aging, 30*(10), 1657-1676.

Knauff, M., Mulack, T., Kassubek, J., Salih, H. R., & Greenlee, M. W. (2002). Spatial imagery in deductive reasoning: a functional MRI study. *Brain Res Cogn Brain Res, 13*(2), 203-212.

Kyllonen, P. C., & Christal, R. E. (1990). Reasoning ability is (little more than) working-memory capacity?! *Intelligence, 14*(4), 389-433.

Li, S.-C., Lindenberger, U., Hommel, B., Aschersleben, G., Prinz, W., & Baltes, P. B. (2004). Transformations in the couplings among intellectual abilities and constituent cognitive processes across the life span. *Psychological Science, 15*(3), 155-163.

Lindenberger, U., & Pötter, U. (1998). The complex nature of unique and shared effects in hierarchical linear regression: Implications for developmental psychology. *Psychological Methods, 3*(2), 218-230.

Lindenberger, U., Von Oertzen, T., Ghisletta, P., & Hertzog, C. (2011). Cross-sectional age variance extraction: what's change got to do with it? *Psychology and aging, 26*(1), 34.

Luo, Q., Perry, C., Peng, D., Jin, Z., Xu, D., Ding, G., et al. (2003). The neural substrate of analogical reasoning: an fMRI study. *Brain Res Cogn Brain Res, 17*(3), 527-534.

Masunaga, H., Kawashima, R., Horn, J. L., Sassa, Y., & Sekiguchi, A. (2008). Neural substrates of the topology test to measure fluid reasoning: An fMRI study. *Intelligence, 36*(6), 607-615.

Maxwell, S. E., & Cole, D. A. (2007). Bias in cross-sectional analyses of longitudinal mediation. *Psychological methods, 12*(1), 23.

McArdle, J. J., Ferrer-Caja, E., Hamagami, F., & Woodcock, R. W. (2002). Comparative longitudinal structural analyses of the growth and decline of multiple intellectual abilities over the life span. *Dev Psychol, 38*(1), 115-142.

McArdle, J. J., Hamagami, F., Meredith, W., & Bradway, K. P. (2000). Modeling the dynamic hypotheses of Gf–Gc theory using longitudinal life-span data. *Learning and Individual Differences, 12*(1), 53-79.

Miyashita, Y. (1993). Inferior temporal cortex: where visual perception meets memory. *Annu Rev Neurosci, 16*, 245-263.

Oldfield, R. C. (1971). The assessment and analysis of handedness: the Edinburgh inventory. *Neuropsychologia, 9*(1), 97-113.

Prabhakaran, V., Smith, J. A., Desmond, J. E., Glover, G. H., & Gabrieli, J. D. (1997). Neural substrates of fluid reasoning: an fMRI study of neocortical activation during performance of the Raven's Progressive Matrices Test. *Cogn Psychol, 33*(1), 43-63.

Rabbitt, P., Diggle, P., Holland, F., & McInnes, L. (2004). Practice and drop-out effects during a 17-year longitudinal study of cognitive aging. *J Gerontol B Psychol Sci Soc Sci, 59*(2), P84-97.

Rabbitt, P., Diggle, P., Smith, D., Holland, F., & Mc Innes, L. (2001). Identifying and separating the effects of practice and of cognitive ageing during a large longitudinal study of elderly community residents. *Neuropsychologia, 39*(5), 532-543.

Radloff, L. S. (1977). The CES-D Scale: A Self-Report Depression Scale for Research in the General Population. *Applied Psychological Measurement, 1*, 385-401.

Raz, N., Ghisletta, P., Rodrigue, K. M., Kennedy, K. M., & Lindenberger, U. (2010). Trajectories of brain aging in middle-aged and older adults: regional and individual differences. *Neuroimage, 51*(2), 501-511.

Raz, N., Gunning-Dixon, F., Head, D., Rodrigue, K. M., Williamson, A., & Acker, J. D. (2004). Aging, sexual dimorphism, and hemispheric asymmetry of the cerebral cortex: replicability of regional differences in volume. *Neurobiol Aging, 25*(3), 377-396.

Raz, N., Gunning, F. M., Head, D., Dupuis, J. H., McQuain, J., Briggs, S. D., et al. (1997). Selective aging of the human cerebral cortex observed in vivo: differential vulnerability of the prefrontal gray matter. *Cereb Cortex, 7*(3), 268-282.

Raz, N., & Lindenberger, U. (2011). Only Time Will Tell: Cross-Sectional Studies Offer No Solution to the Age-Brain-Cognition Triangle: Comment on Salthouse (2011). *Psychological Bulletin, 137*(5), 790-795.

Raz, N., Lindenberger, U., Rodrigue, K. M., Kennedy, K. M., Head, D., Williamson, A., et al. (2005). Regional brain changes in aging healthy adults: general trends, individual differences and modifiers. *Cereb Cortex, 15*(11), 1676-1689.

Raz, N., & Rodrigue, K. M. (2006). Differential aging of the brain: patterns, cognitive correlates and modifiers. *Neurosci Biobehav Rev, 30*(6), 730-748.

Resnick, S. M., Pham, D. L., Kraut, M. A., Zonderman, A. B., & Davatzikos, C. (2003). Longitudinal magnetic resonance imaging studies of older adults: a shrinking brain. *J Neurosci, 23*(8), 3295-3301.

Reuter, M., & Fischl, B. (2011). Avoiding asymmetry-induced bias in longitudinal image processing. *Neuroimage, 57*(1), 19-21.

Reuter, M., Rosas, H. D., & Fischl, B. (2010). Highly accurate inverse consistent registration: a robust approach. *Neuroimage, 53*(4), 1181-1196.

Reuter, M., Schmansky, N. J., Rosas, H. D., & Fischl, B. (2012). Within-subject template estimation for unbiased longitudinal image analysis. *Neuroimage*.

Roca, M., Parr, A., Thompson, R., Woolgar, A., Torralva, T., Antoun, N., et al. (2010). Executive function and fluid intelligence after frontal lobe lesions. *Brain, 133*(Pt 1), 234-247.

Salat, D. H., Buckner, R. L., Snyder, A. Z., Greve, D. N., Desikan, R. S., Busa, E., et al. (2004). Thinning of the cerebral cortex in aging. *Cereb Cortex, 14*(7), 721-730.

Salthouse, T. A., & Meinz, E. J. (1995). Aging, inhibition, working memory, and speed. *J Gerontol B Psychol Sci Soc Sci, 50*(6), P297-306.

Salthouse, T. A., Schroeder, D. H., & Ferrer, E. (2004). Estimating retest effects in longitudinal assessments of cognitive functioning in adults between 18 and 60 years of age. *Dev Psychol, 40*(5), 813-822.

Schretlen, D., Pearlson, G. D., Anthony, J. C., Aylward, E. H., Augustine, A. M., Davis, A., et al. (2000). Elucidating the contributions of processing speed, executive ability, and frontal lobe volume to normal age-related differences in fluid intelligence. *J Int Neuropsychol Soc, 6*(1), 52-61.

Spearman, C. (1904). " General Intelligence," Objectively Determined and Measured. *The American Journal of Psychology, 15*(2), 201-292.

Spearman, C. (1927). *The abilities of man*. New York: Macmillan.

Tarr, M. J., & Gauthier, I. (2000). FFA: a flexible fusiform area for subordinate-level visual processing automatized by expertise. *Nat Neurosci, 3*(8), 764-769.

Turken, A. U., & Swick, D. (1999). Response selection in the human anterior cingulate cortex. *Nat Neurosci, 2*(10), 920-924.

Unsworth, N., Miller, J. D., Lakey, C. E., Young, D. L., Meeks, J. T., Campbell, W. K., et al. (2009). Exploring the relations among executive functions, fluid intelligence, and personality. *Journal of Individual Differences, 30*(4), 194.

Wechsler, D. (1958). *The Measurement and Appraisal of Adult Intelligence* (4 ed.). Baltimore, MD: Williams & Witkins.

Woolgar, A., Parr, A., Cusack, R., Thompson, R., Nimmo-Smith, I., Torralva, T., et al. (2010). Fluid intelligence loss linked to restricted regions of damage within frontal and parietal cortex. *Proc Natl Acad Sci U S A, 107*(33), 14899-14902.

Yuan, P., & Raz, N. (2014). Prefrontal cortex and executive functions in healthy adults: A meta-analysis of structural neuroimaging studies. *Neurosci Biobehav Rev, 42C*, 180-192.

ABSTRACT

LONGITUDINAL CHANGE IN REGIONAL CORTICES AND FLUID INTELLIGENCE

by

PENG YUAN

December 2014

Advisor: Dr. Naftali Raz

Major: Psychology

Degree: Doctor of Philosophy

Fluid intelligence (G*f*) and crystalized intelligence (G*c*) are two factors of the general intelligence. They have distinct age-related trajectories of change. Jung and Haier proposed Parieto-Frontal Integration Theory (P-FIT, 2007) to account for the inter-person variance in reasoning intelligence. Some brain regions such as prefrontal, parietal, temporal and anterior cingulate cortices were included in the P-FIT model and were hypothesized to be involved in fluid reasoning task. Therefore, in the current study, we examined latent growth curves (LGC) of longitudinal change in G*f*, G*c*, prefrontal cortex, parietal cortex, anterior cingulate, temporal cortex and primary visual cortex. Forty-six healthy middle-aged and older adults were involved in baseline assessment. In addition, there were 3 follow-ups, and each of the 46 participants returned back for at least one follow-up. We observed longitudinal decline in G*f*, which accelerated with advanced age. We proposed that the acceleration of G*f* decline could be explained by age-related slowing. Intra-person longitudinal shrinkage was observed in the cortical thickness and volume of prefrontal, parietal, anterior cingulate and temporal cortices, but not in primary visual cortex. Furthermore, longitudinal shrinkage of surface area was

observed in all the examined regions, including prefrontal, parietal, anterior cingulate, temporal and primary visual cortices, although the surface areas at baseline were not correlated with age. Nevertheless, no association was found between the parameters of cognitive change and parameters of cortical change.

AUTOBIOGRAPHICAL STATEMENT

Education:

2014 Ph.D. in psychology, Wayne State University

2012 M.A. in psychology, Wayne State University

2004 B.S. in biology, University of Science and Technology of China

Publications:

Yuan, P., & Raz, N. (2014). Prefrontal cortex and executive functions in healthy adults: A meta-analysis of structural neuroimaging studies. *Neuroscience and Biobehavioral Reviews*, 42, 180-192.

Yuan, P., Daugherty, A. M., & Raz, N. (2014). Turning bias in virtual spatial navigation: age-related differences and neuroanatomical correlates. *Biological Psychology*, 96, 8-19.

Daugherty, A., **Yuan, P.**, Dahle, C., Bender, A., Yang, Y., & Raz, N. Path Complexity in Virtual Water Maze Navigation: Differential Associations with Age, Sex, and Regional Brain Volume. *Cerebral Cortex*, (in press).

Persson, N., Ghisletta, P., Dahle, C., Bender, A., Yang, Y., **Yuan, P.**, Daugherty, A., & Raz, N. Regional Brain Shrinkage over Two Years: Individual Differences and Effects of Pro-Inflammatory Genetic Polymorphisms. *NeuroImage,* (in press).

Zhang, P., Chen, X., **Yuan, P**., Zhang, D., & He, S. (2006). The effect of visuospatial attentional load on the processing of irrelevant acoustic distractors. *Neuroimage*, 33(2), 715-724.

Daugherty, A., Bender, A., **Yuan, P.**, & Raz, N. Changes in Search Path Complexity and Length during Learning of a Virtual Water Maze: Age Differences and Differential Associations with Hippocampal Subfields Volumes, (submitted).